Catalysis Today 154 (2010) 162–182

Contents lists available at ScienceDirect

Catalysis Today

journal homepage: www.elsevier.com/locate/cattod

Deactivation of cobalt based Fischer–Tropsch catalysts: A review

Nikolaos E. Tsakoumis [a], Magnus Rønning [a], Øyvind Borg [b], Erling Rytter [a,b], Anders Holmen [a,*]

[a] Department of Chemical Engineering, Norwegian University of Science and Technology (NTNU), NO-7491 Trondheim, Norway
[b] Statoil R&D, Research Centre, Postuttak, NO-7005 Trondheim, Norway

ARTICLE INFO

Article history:
Available online 28 April 2010

Keywords:
Fischer–Tropsch synthesis
Cobalt
Catalyst deactivation
Review

ABSTRACT

To trace the origin of catalyst deactivation is in many cases difficult. It is usually a complex problem where several mechanisms contribute to the loss of activity/selectivity. Low temperature Fischer–Tropsch synthesis (FTS) is a three phase system having a wide range of products and intermediates. Additionally, high partial pressures of steam will arise during reaction. Thus, the chemical environment in the Fischer–Tropsch synthesis reactor encompasses a large number of interacting species which may negatively affect catalytic activity. Furthermore, it is an exothermic reaction and local overheating might occur. Utilization of the produced heat is crucial and the choice of the reactor should be done with respect to the catalyst stability properties. Catalyst deactivation in the Fischer–Tropsch reaction has been a topic of industrial as well as academic interest for many years. The main causes of catalyst deactivation in cobalt based FTS as they appear in the literature are poisoning, re-oxidation of cobalt active sites, formation of surface carbon species, carbidization, surface reconstruction, sintering of cobalt crystallites, metal–support solid state reactions and attrition.

The present study focuses on cobalt catalyzed Fischer–Tropsch synthesis. The various deactivation routes are reviewed, categorized and presented with respect to the most recent literature.

1. Introduction

Modern Fischer–Tropsch technology aims at converting synthesis gas into long-chain hydrocarbons (FT waxes) [1]. A key element in improved Fischer–Tropsch technology is the development of active and stable catalysts with high wax selectivity. Cobalt is considered the most favourable metal for the synthesis of long chain hydrocarbons due to its high activity, high selectivity to linear paraffins and low water–gas shift (WGS) activity. The catalyst usually consists of Co metal particles dispersed on an oxide support. The Fischer–Tropsch synthesis (FTS) can be described by a chain growth mechanism where a C_1 unit is added to a growing chain. α-olefins and paraffins are the primary products of the synthesis. α-olefins can also participate in secondary reactions adding complexity to the reaction network. For cobalt catalysts oxygen is rejected as water which has a large effect on the activity and selectivity [2]. A number of oxygenates will be produced as well. N_2, CH_4 and CO_2 that may be present in the feed are usually regarded as inert [3].

Catalyst deactivation is a major challenge in cobalt based Fischer–Tropsch synthesis. Combined with the relatively high price of cobalt, improved stability of the catalyst will add competitiveness to the technology. Activity measurements in a demonstration plant have shown that two apparent regimes of deactivation exist [4]. The first initial deactivation regime (period A in Fig. 1) has been linked with reversible deactivation and lasts for a few days to weeks. The second long-term deactivation regime (period B in

Abbreviations: AES, Auger electron spectroscopy; AFM, atomic force microscopy; ASAXS, anomalous small angle X-ray scattering; BET, Brunauer–Emmett–Teller; CSTR, continuous stirred tank reactor; DFT, density functional theory; DOR, degree of reduction; DOS, density of states; DRIFTS, diffuse reflectance infrared Fourier transform spectroscopy; EDS, energy dispersive spectroscopy; EELS, electron energy loss spectroscopy; EF-TEM, energy filtered-transmission electron microscopy; EXAFS, extended X-ray absorption fine structure; *fcc*, face centered cubic; FT(S), Fischer–Tropsch (synthesis); GHSV, gas hourly space velocity; *hcp*, hexagonal close packed; HFS-LCAO, Hartree–Fock–Slater linear combination of atomic orbitals; HR-TEM, high resolution-transmission electron microscopy; HS-LEIS, high sensitivity-low energy ion scattering; HAADF, high angle annular dark field; ICP, inductively coupled plasma; IR, infrared; MES, Mössbauer emission spectroscopy; MS, mass spectrometer; NEXAFS, near-edge X-ray absorption fine structure; PM-RAIRS, polarization modulation-reflection absorption infrared spectroscopy; ppb, parts per billion; ppm, parts per million; RBS, Rutherford backscattering spectrometry; ROR, reduction–oxidation–reduction; rpm, revolutions per minute; SBCR, slurry bubble column reactor; SIMS, secondary ion mass spectrometry; SSITKA, steady state isotopic transient kinetic analysis; STM, scanning tunneling microscopy; STP, standard temperature and pressure; TEM, transmission electron microscopy; TGA, thermogravimetric analysis; TOS, time on stream; TPD, temperature programmed desorption; TPO, temperature programmed oxidation; TPH, temperature programmed hydrogenation; TPR, temperature programmed reduction; UBI-QEP, unity bond index-quadratic exponential potential; UHV, ultra high vacuum; WGS, water–gas shift; XANES, X-ray absorption near edge structure; XAS, X-ray absorption spectroscopy; XPS, X-ray photoelectron spectroscopy; XRD, X-ray diffraction.

* Corresponding author. Tel.: +47 91897164.
E-mail address: holmen@chemeng.ntnu.no (A. Holmen).

0920-5861/$ – see front matter © 2010 Elsevier B.V. All rights reserved.
doi:10.1016/j.cattod.2010.02.077

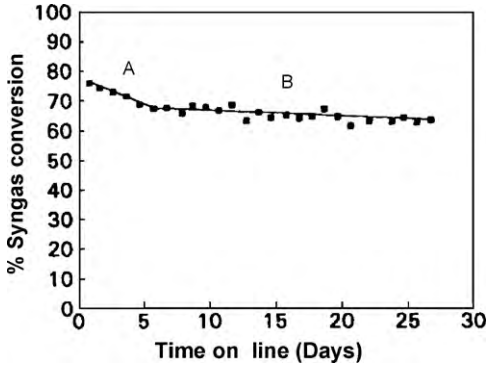

Fig. 1. Common deactivation profile for cobalt catalysts in FTS. Adapted from reference [4].

Fig. 1) is associated with irreversible deactivation and has therefore operational significance. This change in deactivation rate with time on stream suggests that the actual cause of deactivation is not the result of one, but a combination of several phenomena.

The proposed mechanisms of catalyst deactivation include poisoning, sintering, surface carbon formation, carbidization, cobalt re-oxidation, cobalt–support mixed compound formation, surface reconstruction and mechanical deactivation through attrition. The Fischer–Tropsch catalysts are usually very sensitive to poisoning and purification of the synthesis gas is therefore an important part of the process, particularly for processes using coal and biomass as feedstocks [5]. The loss of activity is also related to process conditions such as temperature, pressure, conversion, partial pressures of synthesis gas and steam and the type of reactor (fixed-bed or slurry). Hence, reproduction of a realistic FT environment in deactivation studies is fundamental.

The study of catalyst deactivation is mainly a characterization oriented problem. Spent catalyst has to be characterized and compared with its activated counterpart. A main challenge for studying catalyst deactivation in FTS is the fact that the catalyst is embedded in wax after use. The wax limits the range of technique that can be applied for characterization of the spent catalysts. In addition, the sensitivity of the active phase against air hampers the handling of the dewaxed catalysts. Deactivation is an inevitable phenomenon in FTS although catalytic systems show different behaviour. Regeneration is therefore also an important topic.

2. Causes of catalyst deactivation in Fischer–Tropsch synthesis

In the following paragraphs the main mechanisms of catalyst deactivation in FTS are discussed.

2.1. Poisoning

2.1.1. Sulphur compounds

Sulphur is a known poison for metals since it adsorbs strongly on catalytically active sites. The consequences of this strong bonding are usually a physical blocking of the sites and possibly the electronic modification of neighbouring atoms [6]. For cobalt FT catalysts poisoning by sulphur appears to be more a geometric blockage of sites than an electronic modification. It has been reported that one sulphur atom adsorbed on a Co/Al_2O_3 catalyst poisons more than two cobalt atoms [7]. Sulphur is usually present in the feed and is therefore considered as a potential cause of deactivation. Raw synthesis gas derived from biomass or coal will usually contain significant amounts of sulphur, whereas sulphur usually is removed from natural gas before the reformer section. Sulphur may also stem from corrosion inhibitors which are occasionally added. In any case, there is a possibility that traces of sulphur can reach the FTS reactor, typically during operational upsets. Thus, already at the early stages of the development of the FT technology, the effect of sulphur in different molecular forms was studied [8]. An upper limit of sulphur concentration in the feed was proposed already by Fischer (1–2 mg/m^3) [9]. However, these limits are decreased and usually kept below 0.02 mg/m^3 in today's applications [10].

The oil crisis in the 70 s raised crude oil prices and hence renewed the interest in FTS mainly using natural gas as feedstock. This resulted in increased research and process development in the field of cobalt based FTS. Madon and Seaw summarized in 1977 the literature concerning the effect of sulphur [9]. In particular they presented several studies carried out for more than four decades dealing with sulphur effects on different FT catalysts. For cobalt catalysts the results seemed to agree that sulphur, added in low concentrations in the forms of H_2S and CS_2, has a promotional effect on the catalysts. In particular, at low concentrations of sulphur, an increase in the catalysts lifetime and also the selectivity towards heavier hydrocarbons was observed. Further addition of sulphur compounds led to complete catalyst deactivation.

Studying sulphur poisoning by *in situ* methods is challenging. H_2S, which is normally being used as a sulphur carrier, adsorbs strongly on metallic tubes. In addition, it is corrosive, toxic and flammable. The selection of sulphur carrier is important since there is a significant difference between adsorption phenomena of organic (e.g. C_2H_5SH) and inorganic (e.g. H_2S) sulphur containing molecules. A proper sampling procedure is essential for the accuracy of such studies, due to an expected intraparticle and reactor poisoning gradient (especially for plug flow reactors) [11,12].

Bartholomew and Bowman [13] studied the effect of sulphur by introducing 0.5–8 ppm H_2S in the reactor feed through Teflon lines. For the silica-supported cobalt catalyst a decline in catalyst activity was observed for the entire range of sulphur content in the feed. The decline appeared to be more intense for concentrations between 0.5 and 2 ppm, while less for 5–6 ppm of H_2S. A possible explanation for this trend was that at higher sulphur concentrations a surface sulphide of a different structure or multilayers of sulphide were created. Catalyst selectivity was also altered as a result of sulphur addition leading to increased production of heavier hydrocarbons ($>C_4$). A possible reason for the increased selectivity to higher molecular weight products could be the selective adsorption of the H_2S on sites which normally adsorb hydrogen, resulting in a hydrogen deficient surface. Decreased water production, which is a result of the lower conversion, normally affects the product distribution in the opposite direction. Chaffee et al. also studied *in situ* sulphur poisoning using H_2S as the sulphur carrier in a fixed-bed reactor [14]. Commercial catalysts were used and the main focus of the study was on the effect of the H_2/CO ratio on the catalyst deactivation behaviour. The result showed that for cobalt catalysts, H_2 rich feeds appeared to be more sensitive to sulphur poisoning than lower H_2/CO ratios. Furthermore, 300 ppm H_2S in the feed had minor impact on the product selectivities, but in most cases it favoured the formation of methane and saturated products.

Due to the difficulty that arises when studying sulphur poisoning by *in situ* techniques, the effect of sulphur poisoning has mainly been investigated by *ex situ*, "pre-sulphidation" procedures. Coville and co-workers have studied extensively the effect of sulphur addition during catalyst preparation [15–17]. These studies also included the effect of additives such as boron and zinc, which act as sulphur sinks. Results from diffuse reflectance infrared Fourier transformed spectroscopy (DRIFTS) and temperature programmed reduction (TPR) that were carried out on TiO_2 and SiO_2 supported cobalt catalysts, showed that in the entire range of sulphur loading (100–2000 ppm) CO adsorption inhibition is being observed. In addition, in the range of 200–2000 ppm sulphur, an increase in the reduction temperature of the sulphided samples was detected.

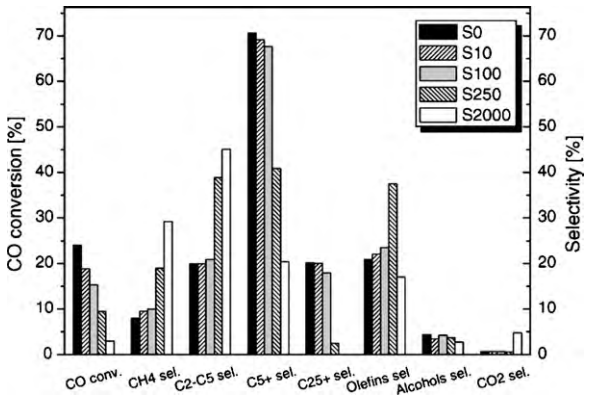

Fig. 2. CO conversion and selectivities to the main products obtained with different sulphured catalysts. Experimental conditions: catalyst loading 3 g diluted 1:2 (v/v) with α-Al_2O_3, T_{cat} = 220 °C, P = 20 bar, H_2/CO inlet molar ratio = 2, GHSV = 5000 N cm^3/h/gcat.
Adapted from reference [18].

Further studies of the catalyst activity by IR suggested that the sulphur loading had a promotional effect for concentrations lower than 200 ppm. At such concentrations an increase in the catalyst activity and selectivity towards methane was observed [15]. By using $(NH_4)_2S$ as the sulphur source for a boron treated catalyst, Li and Coville showed that the additive did not influence the catalyst resistance to sulphur at low concentrations (100 and 200 ppm). However, at higher loadings (500 ppm) the reaction rate was twice as high as compared to the boron-free catalyst with the same sulphur loading. The selectivity was also influenced by sulphur, leading to a lower chain growth probability α. Boron was selected because of its electron accepting nature which neutralizes the electronic density introduced by sulphur addition (sulphide ions are considered as electron donors). Recently, the effect of zinc as an additive has been reported showing the importance of the step in which sulphur is being introduced to the system during the presulphidation procedure [17]. Sulphided zinc-containing Co/TiO_2 catalyst showed about 45% improved activity compared to sulphided catalyst without zinc. In both cases sulphur and zinc were introduced before cobalt. In agreement with previous results the selectivity for the sulphided catalyst was shifted towards lighter hydrocarbons.

Visconti et al. recently reported on the effect of sulphur poisoning of a γ-Al_2O_3 supported Co catalyst [18]. Sulphur in the range of 0–2000 ppm was added *ex situ* to the catalyst by incipient wetness impregnation of ammonium sulphide. This range corresponds to approximately 50.000 h on stream, assuming that the feedstock contains 0.02 mg/m^3 of sulphur and a space velocity of 2000 cm^3 (STP)/h/gcat. The catalysts reducibility, activity, hydrogenation ability and selectivity were experimentally estimated. The results showed no morphological changes in the catalyst structure. However, in the entire range of sulphur addition, a negative effect on the catalysts reducibility and the catalytic activity was observed. The effects were more pronounced at higher loadings (Fig. 2). At the same time the product selectivity shifted towards lighter hydrocarbons and CO_2 production. The results are suggesting selective poisoning by sulphur atoms having different influence at different loadings. An attempt to model the sulphur effect on the conversion rate was also presented.

The results reveal a mismatch between the static *ex situ* and dynamic *in situ* experiments as expected. The *ex situ* studies agree that sulphur addition influences the reducibility, activity and selectivity of the catalyst shifting it to lighter hydrocarbons. The promotional effect of small amounts of sulphur is more controversial.

2.1.2. Nitrogen compounds

Little is known on the effect of nitrogen containing compounds and the available information is mainly found in patents. Leviness et al. investigated the effects of NH_3, HCN, and NO_x [19]. Such compounds are usually present downstream of the synthesis gas generation processes. It was found that small amounts of the N-contaminants (even in ppb levels) have an immediate effect on the catalysts activity. Extended operation under such conditions showed a direct correlation between nitrogen compound concentrations and the deactivation rate. However, the deactivation appears to be reversible and a mild *in situ* hydrogen treatment can recover 100% of the catalyst activity. A reduction of the amount of N-contaminants in the feed to less than 50 ppb is proposed [20].

2.1.3. Alkali and alkaline earth metals

It is known that small amounts of alkali metals, i.e. Na, K, Li, usually can change the catalyst behaviour in Fischer–Tropsch synthesis [21,22]. The chain growth probability increases significantly with alkali metal addition, while the activity is negatively influenced. It is suggested that for any alkali metal promoter there is an optimum concentration level that balances catalyst activity and promotional effects [21,23]. Alkali metals are present in low quantities in most common supports and sodium appears to have a detrimental effect on FT activity [24]. Apparently, poisoning by alkali metals is not an operational deactivation mechanism. Nevertheless, care should be taken when choosing raw materials for catalyst preparation. The effect of alkali metals seems to be more pronounced with biomass as the raw material [25].

2.2. Sintering of cobalt crystallites

Sintering leads to a reduction of the active surface area. Sintering is thermodynamically driven from the, energetically favoured, surface energy minimization of the crystallites. In addition, the size dependent mobility of the crystals on various supports contributes significantly to the sintering behaviour. Strongly interacting supports like Al_2O_3 are retarding crystallite diffusion. Two main mechanisms of sintering exist: (a) atomic migration (Ostwald ripening or coarsening) and (b) crystallite migration (coalescence). High temperatures and water vapour (hydrothermal conditions) accelerate the process [6]. Sintering in general is considered to be an irreversible phenomenon. However, by a reduction–oxidation–reduction (ROR) sequence at certain conditions it may be possible for cobalt to regain dispersion [26]. This redispersion process seems to be assisted by the nanoscale Kirkendall effect [27,28]. Although redispersion through the ROR treatment results in a catalyst with similar initial activity, a higher deactivation rate is usually, [29] but not always observed.

The most common techniques for detecting sintering are X-ray diffraction (XRD), transmission electron microscopy (TEM) and H_2 chemisorption. Extended X-ray absorption fine structure (EXAFS) and anomalous small angle X-ray scattering (ASAXS) are gaining importance in crystallite size analysis as synchrotron based techniques with *in situ* capabilities are readily available. However, the previously mentioned techniques are covering different size ranges and are not always applicable.

FTS is a highly exothermic reaction and the potential for sintering is therefore relatively high. Special attention should therefore be given to the choice of reactor, since isothermal conditions are important. Fixed-bed reactors have poor heat transfer rates and hot spots may arise during operation [12]. However, with proper design and the use of multitubular fixed-bed reactors these limitations can be overcome [30]. Slurry reactors have the advantage of isothermal conditions due to a higher heat transfer coefficient [31].

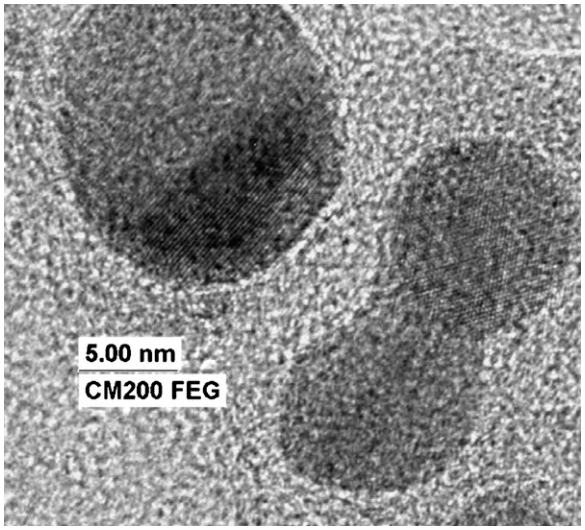

Fig. 3. TEM image of two cobalt particles during coalescence. Adapted from reference [40].

Cobalt crystallites used in FT catalysts usually have a diameter of a few nanometres (3–20 nm) [32]. It is expected that their physicochemical properties differ from those of the bulk metal. In particular the melting point of nanoparticles is crucial for their diffusion rates and can deviate significantly from the bulk. At temperatures near the melting point, the diffusion becomes faster and the probability of two crystallites to collide is higher. This theory is further supported by the fact that the Hüttig temperature for bulk cobalt is 253 °C, not far from low temperature FT conditions [33]. Furthermore, the mobility of the crystals may be affected by the crystal structure and the nature of the site, with low coordinated metals atoms being more mobile [34,35].

Sintering has been proposed as a reason for FT catalyst deactivation already by Fischer and Tropsch. A magnesium promoter was incorporated in order to inhibit the effect [36,37]. Since the early works by Fischer and Tropsch, many reports have linked deactivation with sintering as described below.

Sintering of cobalt crystallites may be accelerated in the presence of water [6]. A number of studies related to the effect of water in the catalyst deactivation of FTS, suggest sintering of cobalt crystallites as one of the main deactivation mechanisms. Bertole et al. investigated the effect of water using a rhenium promoted unsupported cobalt catalyst [38]. They showed that the periodic addition of water at 210 °C and high partial pressures (4 and 8 bar) resulted in a permanent loss of activity (starting conditions 10 bar H_2, 5 bar CO, 8 bar inert and ~11% CO conversion). A subsequent hydrogen treatment recovered only 80% of the activity. The CO adsorption capability of the catalyst was reduced which supports the hypothesis of loss of active surface area due to sintering of cobalt crystals. Recent studies by Kiss et al. point to sintering as an indirect deactivation mechanism [29]. It appears that crystallite growth occurs as a consequence of re-oxidation of cobalt crystallites (see Section 2.4 below). The work by ExxonMobil [29,39,40] has been performed in a variety of reactors (fixed-bed and slurry) involving TGA (thermogravimetric analysis), chemisorption and (transmission electron microscopy) TEM as the characterization techniques. The used samples were treated and analyzed *ex situ*. TEM images indicated sintering of cobalt crystallites. The authors proposed coalescence (crystallite migration) as the predominant sintering mechanism as indicated in Fig. 3. In addition, agglomeration seemed to occur for a critical distance between the cobalt crystallites.

XRD and H_2 chemisorption studies of silica-supported Co/ZrO_2 catalyst before and after FTS by Sun and co-workers [41,42] showed that sintering contributes to the deactivation of the catalyst. The experiments were performed in a laboratory fixed-bed reactor at 200 and 210 °C, 20 bar and $H_2/CO = 1$, 2 and 3. Addition of water during reaction led to sintering of the cobalt crystallites. The results of different synthesis gas ratios suggested that sintering was detectable only for the lowest H_2/CO ratio. The XRD and H_2 chemisorption results were supported by dispersion measurements from X-ray photoelectron spectroscopy (XPS).

In a study of potential offshore application of FTS, different compositions of synthesis gas were tested over a silica-supported cobalt catalyst also containing ThO_2 and MgO (220 °C, 20 bar, GHSV = 250 h^{-1} and $H_2/CO = 2.1$) [43]. The feedstock contained different amounts of nitrogen and carbon dioxide, simulating offshore FTS conditions. Hydrogen chemisorption on spent catalysts showed sintering of the cobalt crystallites and it appeared to be more delayed for nitrogen rich feeds.

The sintering behaviour of a calcined and an uncalcined SiO_2 supported cobalt catalyst was investigated by Bian et al. [44]. The catalysts were exposed to synthesis gas in a fixed-bed reactor for 60 h at 10 bar, 200–240 °C and CO conversion up to 90%. Both catalysts were characterized by XRD, EXAFS and H_2 chemisorption before and after reaction. As expected the uncalcined catalyst was more sensitive to sintering whereas the calcined catalyst displayed only minor changes in crystallite size. However, increasing the temperature to 240 °C accelerated the growth of cobalt crystallites, especially for a catalyst containing small (6–10 nm) cobalt crystallites.

Davis and co-workers have studied alumina supported cobalt catalysts promoted with platinum and ruthenium [45,46]. Three catalysts were tested in a continuous stirred tank reactor (CSTR) at 220 °C, 18 bar, $H_2/CO = 2$ and 750 rpm. The catalysts were unloaded from the reactor after reaction and characterized. The alumina supported catalysts contained 15 wt% cobalt and promoter concentrations of 0.5 wt% Pt, 0.5 wt% Ru and no promoter. The unloaded samples were studied by EXAFS and spectra were compared with acquired data from a cobalt foil and fresh passivated catalysts. Results derived from the k^3 weighted Fourier transformation showed that there was an increase in the Co–Co coordination, a fact that suggests sintering of the cobalt clusters. However, it is emphasized that the fresh passivated sample contains a fraction of CoO according to X-ray absorption near edge structure (XANES) data. Thus, the Co–Co coordination will be smaller compared to a completely reduced catalyst. Das et al. [47] also examined a cobalt based γ-Al_2O_3 supported catalyst having different amounts of rhenium (0, 0.2, 0.5 and 1 wt%) and crystallites in the range of 5–7 nm. The 0.2 wt% Re-15 wt% Co/γ-Al_2O_3 catalyst was tested in a CSTR and samples were removed at different times on stream. EXAFS data analysis indicated an increase in the cobalt cluster size with time on stream. This was based on the slightly increased Co–Co coordination number. It appears that the use of noble metals as promoters enhances the reducibility of the cobalt and thus increases the number of active sites. Accordingly, it is likely that small crystallites of an unpromoted catalyst that would be difficult to reduce at the applied conditions are reduced with the assistance of the promoter. These small crystallites are more sensitive to sintering and other phenomena that may lead to deactivation, e.g. re-oxidation and solid state reactions with the support. This sensitivity of the smaller clusters leads to higher rates of initial deactivation for the promoted catalysts. However, it should be mentioned that EXAFS is regarded as a supplementary technique for size estimation of clusters containing more than 1200 atoms (approximately 4–5 nm). Beyond this range XRD and TEM are considered as more accurate [48].

Multiple oxidation–reduction cycles have also been performed in order to simulate extended ageing of the catalyst [49]. A

2 wt% Ru-promoted 15 wt% Co/Al_2O_3 catalyst was tested and batches of the catalyst underwent different cycles of an oxidation (calcination)–reduction procedure. Subsequently, a number of those batches were tested in a CSTR using a Polywax-3000 solvent at 220 °C, 19.3 bar, $H_2/CO = 2$, 750 rpm and CO% conversion of 55–60%. XANES/EXAFS, TPR, HR-TEM, and EDS elemental mapping techniques were employed in order to study changes in the samples after the different treatments. It appears that the oxidation–reduction treatments led to sintering of the metallic cobalt clusters.

Tavasoli et al. [50,51] concluded that catalyst deactivation is related to sintering at low steam partial pressures where the effect of water-induced oxidation is not as severe. Cobalt re-oxidation and formation of mixed metal–support compounds were identified as the main deactivation mechanisms when $P_{H_2O}/(P_{H_2} + P_{CO})$ was above 0.75. Experiments were performed in a laboratory fixed-bed reactor using a Co-Ru/γ-Al_2O_3 catalyst. According to the authors sintering is the main cause of long-term deactivation in FTS and the change in cobalt cluster size can be modelled using a power law expression having a power order of $n = 39.7$ [50]. These results were derived from H_2 chemisorption of a fresh catalyst and catalyst subjected to 220 °C, 20 bar, and a $H_2/CO = 2$ for a period of 850 and 1000 h. Additionally, the increase in the C_{5+} selectivity with time on stream (TOS) supports these results since larger cobalt particles are more selective to higher molecular weight products. Finally, analysis of samples from different parts of the reactor bed showed an increased particle growth towards the reactor outlet. This sintering gradient along the reactor may be due to different partial pressures of steam or temperature gradients along the reactor bed.

Commercial Sasol catalysts containing $Co/Pt/Al_2O_3$ have been studied after use in a SBCR (slurry bubble column reactor) with a capacity of 100-barrel/day working under commercially relevant conditions (230 °C, 20 bar, $H_2/CO \sim 2$) [52]. The samples were periodically unloaded from the reactor, treated in a procedure consisting of xylene extraction followed by hydrocracking, passivated over dry ice and characterized by means of H_2 chemisorption and high angle annular dark field-transmission electron microscopy (HAADF-TEM). Changes in crystal morphology during TOS were clearly evident after 3 days on stream. Crystallite size distributions at different TOS were obtained by size determination of about 1000 crystallites per sample. By ruling out oxidation and fouling as reasons for surface area loss, H_2 chemisorption results were in agreement with TEM observations. It was observed from both techniques that the rate of active surface area loss decreased significantly after 10–20 days on stream. The results clearly suggested that sintering is one of the major mechanisms involved in the initial FT catalyst deactivation. A further attempt to model deactivation showed that sintering appears to be responsible for 40% of the total deactivation observed in FTS.

An *in situ* XRD–XAS approach for studying cobalt crystallite changes during FTS start-up under industrially relevant conditions has recently been published by Rønning et al. [53]. Synchrotron X-ray diffraction was used as a tool for studying *in situ* changes in the crystallite size of a Re-promoted Co/γ-Al_2O_3 catalyst. The reactor cell, proposed by Clausen and co-worker [54], resembles the behaviour of a plug flow reactor. The reaction was carried out for several hours under FT relevant pressures (10 and 18 bar) and temperatures (210 and 400 °C) with a constant H_2/CO ratio of 2.1. Diffractograms were acquired during FTS and the light hydrocarbons were monitored by an on-line mass spectrometer (MS). Line broadening analysis of the XRD profiles suggested that no significant crystallite growth occurred during start-up at 210 °C (Fig. 4). However, increasing the temperature to 400 °C forced Co crystals to sinter resulting in a 20% size increase. These techniques are promising for studying FTS catalysts at their working conditions and could reveal information that will lead to better understanding of deactivation phenomena. Recently Karaca et al. performed an *in situ* synchrotron XRD study by using similar equipment [55]. Alumina supported cobalt catalysts were tested at 210 °C, 20 bar and $H_2/CO = 2$. During the first hours of reaction a crystallite size growth was detected. Line broadening analysis showed that *fcc*-Co crystallite diameters increased from 6 to 10 nm, while subsequently the formation of Co_2C carbide compounds was also detected. According to the authors, cobalt sintering and carbidization (see Section 2.3.1) seem to be the major mechanisms of initial deactivation in FTS.

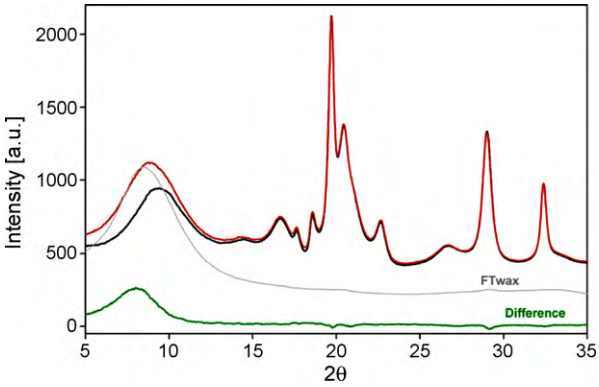

Fig. 4. Diffractograms from the start (black) and after 2 h of FT reaction at 210 °C and 10 bar (red). The difference curve (green) indicates no significant changes in the Co peaks during reaction compared to scattering from FT wax only (gray) and from the catalyst after 2 h of reaction at 210 °C, λ = 0.70417 Å. (For interpretation of the references to color in this figure legend, the reader is referred to the web version of the article.)
Adapted from reference [53].

Furthermore, sintering of the support is possible especially at hydrothermal conditions. However, the phenomenon is rarely observed since FTS is usually performed at rather mild conditions. Sintering of the silica support has been suggested as a cause of deactivation in cobalt based FTS by Huber et al. [56]. High surface area silica-supported catalysts were investigated. Steam treatments of the catalyst at pressures resembling FTS conditions were performed at 220 °C. The treatment led to a significant loss of BET surface area as well as the formation of catalytically inactive cobalt silicates. The pore size distribution and the cobalt hydrogen chemisorption surface area determined by H_2 chemisorption were affected as well. Activity measurements on the same catalysts showed activity loss during time on stream.

2.3. Carbon effects

In general, carbon is known for having positive as well as negative effects in catalysis [6,57]. A detailed classification of carbon species that can be formed on a catalyst surface has been given by Bartholomew [58]. FT synthesis can be described as a polymerization reaction where a C_1 unit is added to a growing chain. Different mechanisms have been proposed based on different C_1 monomers; produced from CO dissociation, H_2 assisted CO dissociation, and molecularly adsorbed CO. In any case, the surface consists of a wide range of carbon containing molecules. Each of those molecules might interact differently with the catalyst. Furthermore, side reactions like the Boudouard (Fig. 5) reaction may enhance carbon formation. It is therefore reasonable to expect that carbon is a possible cause of deactivation since carbon may interact with the metal under reaction conditions and form inactive species (e.g. bulk or subsurface carbides) or form species that may act as reaction inhibitors (e.g. amorphous, graphitic or other surface carbon species). The possible routes for carbon formation during FTS are presented in Fig. 5 [59]. However, the mechanisms shown in

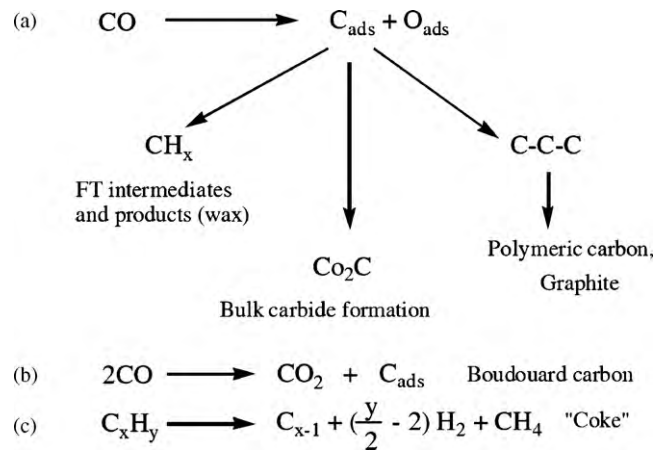

Fig. 5. Possible carbon formation routes on cobalt based catalysts during Fischer–Tropsch synthesis.
Adapted from reference [59].

Fig. 5 are mostly related to hydrogen deficient conditions and do not take into account that the reaction usually is carried out at a H_2/CO ratio close to 2.

FTS has been classified as a carbon (coke) insensitive reaction [57]. The presence of hydrogen and the hydrogenation function of the catalyst should not allow carbon to accumulate on the surface. Accordingly, coke precursors may rapidly transform to hydrocarbons and are thus considered as reaction intermediates. In spite of the above statement, several reports have pointed to the possible deactivation by carbon in different forms (polymeric carbon, graphitic carbon, refractory carbon or other carbonaceous species).

Surface carbon is difficult to detect, particularly during or after FTS when the surface is covered with various hydrocarbon products. The most common characterization techniques that have been successfully employed in determining carbon species are temperature programmed techniques [60–62]. In most cases the deactivated catalysts have been hydrogenated at elevated temperatures and the evolution of methane and other products is detected. The carbon species are evaluated according to their hydrogenation resistance. Recently, more advanced techniques like energy filtered-transmission electron microscopy (EF-TEM) and high sensitivity-low energy ion scattering (HS-LEIS) [61] have been applied to dewaxed samples. Auger electron spectroscopy (AES) and X-ray photoelectron spectroscopy have also been used although to a lesser extent. For bulk carbide detection XRD remains the most commonly applied technique [63,64]. However, Co_xC carbides appear to be metastable, especially in presence of H_2, [65] and rarely observed by *ex situ* techniques [66].

2.3.1. Bulk carbide formation

Cobalt crystallites are more resistant to carbide formation than iron partly because carbon diffusion rates in cobalt are lower by a factor of 10^5 [67]. In addition, the calculated heat of chemisorption of atomic carbon by using the UBI-QEP method is weaker for cobalt (162 kcal/mol) than iron (200 kcal/mol) suggesting a lower possibility of bulk carbide formation in cobalt catalysts [68,69]. However, cobalt crystallites subjected to pure carbon monoxide at atmospheric pressure at 226–230 °C slowly form a cobalt carbide corresponding to Co_2C [63]. Fischer and Tropsch were the first suggesting that cobalt carbide may be a reaction intermediate [70]. However, later studies clarified that this carbide is not bulk cobalt carbide, but probably a surface species [71,72].

Recently, it was shown that hydrogen treatments, at low temperature, are leading to the decomposition of bulk cobalt carbide and primarily creation of the hexagonal close packed (*hcp*) cobalt structure [73]. This structure appears to be more active in FTS [74]. The transformation of the face center cubic (*fcc*) cobalt phase to carbide seems to be more difficult. From the above it is expected that FT catalysts that have been deactivated due to carbide formation, after mild hydrogen treatment at low temperatures, will have higher content of the *hcp* cobalt structure and hence regaining the initial activity. However, no such change in the cobalt phase has been reported.

Although the probability of bulk carbide formation in cobalt based FTS is low, some studies have reported the detection of Co_2C in used catalyst or by *in situ* characterization. Agrawal et al. studied CO hydrogenation on cobalt, supported on α-Al_2O_3 plates [75]. A quartz internal-recycle reactor was used and operated under methanation conditions (>90% CH_4 selectivity, 200–400 °C, atmospheric pressure and 0.1–20% CO in H_2). The spent catalysts were characterized with AES. It appears that under those conditions carbon monoxide is being dissociated on the surface and the resulting surface carbon species can be hydrogenated to form methane or diffuse into the bulk and form carbides or surface graphitic species. The authors suggested that carbidization of bulk cobalt and the formation of graphitic carbon on the Co surface are responsible for the observed catalyst deactivation [75].

A direct link between FT catalyst deactivation and bulk carbide formation has also been proposed by Ducreux et al. [64]. Different catalysts, i.e. Co/Al_2O_3, Co/SiO_2 and $Co\text{-}Ru/TiO_2$ were studied at 230 °C, 3 bar, $H_2/CO = 9$ and CO conversion ~20% and characterized by *in situ* XRD. The observed catalyst deactivation was different for the various catalysts. Simultaneously with this activity decline, new diffraction peaks appeared corresponding to Co_2C. This phenomenon was observed only for TiO_2 and Al_2O_3 supported catalysts, whereas no Co_2C formation was observed on SiO_2 supported catalyst. The activity decline could be directly correlated to carbide formation.

Jacobs et al. studied the effect of promoters in FTS on a 15 wt% Co/Al_2O_3 catalyst [46] claiming evidence of carbide formation. The X-ray diffraction data from a catalyst used in a CSTR (18 bar, 220 °C and $H_2/CO = 2$) suggested the existence of Co_2C. Several of the peaks in the diffractogram correlated well with crystalline Co_2C suggesting that small amounts of Co_2C may have been formed during synthesis. This is in agreement with Tavasoli et al. [50] who also detected Co_2C peaks in the diffractograms of catalysts used in a fixed-bed reactor at 220 °C, 20 bar, and a ratio $H_2/CO = 2$ for a period of 1000 h.

Several other reports also exist claiming the formation of cobalt carbide and examples are Gruver et al. [76] and Karaca et al. [55] on alumina supported catalysts, Xiong et al. [77] on cobalt supported on activated carbon and Pennline and co-workers [78,79] for a bifunctional catalyst containing cobalt-thoria mixed with ZSM-5 and tested with $H_2/CO = 1$.

2.3.2. Fouling by carbon species

Long chain hydrocarbons are the desired products in low temperature Fischer–Tropsch synthesis. FT hydrocarbon waxes are accumulated on the surface can potentially retard the rate of diffusion of the reactants and slow down the reaction [11]. The hydrocarbons are not directly connected to the catalyst deactivation, they are just slowing down an already slow reaction. However, since FTS catalysts are used to produce "syncrude" they are not considered as highly selective systems. They are designed to produce a range of hydrocarbons with carbon numbers that can reach ~100 or more. Therefore, higher molecular weight hydrocarbons, produced from the main or side reactions (e.g. condensations, oligomerizations, cracking), may accumulate and block microporous channels and hence the catalytically active surface. These hydrocarbon species are referred to as polymeric amorphous carbon. In addition, more stable carbon compounds with less hydrogen

content, e.g. coke or graphite-like species may build up on the surface and poison or physically block the active sites. It has been proposed that the above mentioned carbon species are linked with the catalyst deactivation [6,58].

Although FTS has been considered as a coke-insensitive reaction [57], hydrogen deficient conditions may lead to the formation of carbon species. Such conditions may be present in Fischer–Tropsch reactors [41].

Lee et al. have used combined thermogravimetric-temperature programmed reduction and Auger electron spectroscopy to distinguish the forms of carbon produced from CO disproportionation on a reduced Co/Al_2O_3 sample at different temperatures (250–400 °C) [60]. It was suggested that carbon is present in two forms: atomic and polymeric carbon. High temperature led to an increase in the total carbon deposition, but a decrease in the fraction of atomic carbon. Consequently the remaining sample was more resistant to reduction. AES results confirmed the increase in the amount of carbon. From these results, the authors suggested that the carbon species which was difficult to reduce (polymeric and/or graphitic) created a pore diffusion inhibiting effect rather than an electronic modification of the active sites. Small cobalt crystallites seem to be more sensitive to the carbon formation. In addition, activity tests of the carbon deposited samples showed that a higher deposition temperature leads to more deposited carbon and a higher activity loss. This activity loss is followed by a shift in the selectivity towards unsaturated hydrocarbons.

Niemelä and Krause proposed that the initial deactivation, corresponding to the first hour of the reaction, is a result of selective blockage of the most narrow catalyst pores by high molecular weight hydrocarbon species and/or coke [80]. Co/SiO_2 catalysts derived from different precursors were evaluated for their behaviour in FTS for 120 h (fixed-bed reactor, 5 bar, 235–290 °C and $H_2/CO = 3$). Detailed analysis of the FT products (IR and MS analysis) showed that low reaction temperatures enhanced the formation of long chain oxygenate species, mainly alcohols and ketones. These species are reactive and they can assist in the formation of long chain hydrocarbons, e.g. by condensation reactions.

A synergy between poisoning and carbon deposition has also been reported [81]. It is known that poisons, apart from the physical blocking of the active site, may alter electronically the neighbouring atoms due to strong chemisorption (see Section 2.1). This could possibly lead to a change in the properties of the site and hence promote side reactions. Kim et al. studied the effect of sulphur poisoning on the decomposition of ethylene over unsupported cobalt catalyst powders [81]. The cobalt powders were reduced and treated in H_2S. Afterwards, they were subjected to an ethylene/hydrogen mixture (1:1) at 535 °C. The catalyst samples were analyzed with several techniques such as TEM, XRD and gravimetric methods. It was shown that the pretreatment of cobalt with low levels of hydrogen sulphide (4–100 ppm) increased the amount of produced carbon by more than an order of magnitude compared to the untreated catalyst. The carbon filaments deposited on uncontaminated cobalt particles were found to be highly graphitic in nature. On the other hand, higher levels of H_2S (>60 ppm) in the feed or (>500 ppm) during pretreatment completely suppressed catalytic activity. The authors suggested that low levels of sulphur may reconstruct the metal surface in such a way that graphitic carbon formation is enhanced, whereas higher concentrations result in 2D or 3D bulk sulphides. Additionally, it was found that sulphur adatoms induced fragmentation of the cobalt particles. This demonstrates the relation between sulphur poisoning and carbon deposition with redispersion of cobalt particles.

Several studies have also been carried out on catalyst samples obtained from large demonstration units operated for months [61]. Sasol operated a 0.05 wt% Pt-20 wt% $Co/\gamma\text{-}Al_2O_3$ catalyst in a slurry bubble column reactor for 6 months. Catalyst samples were

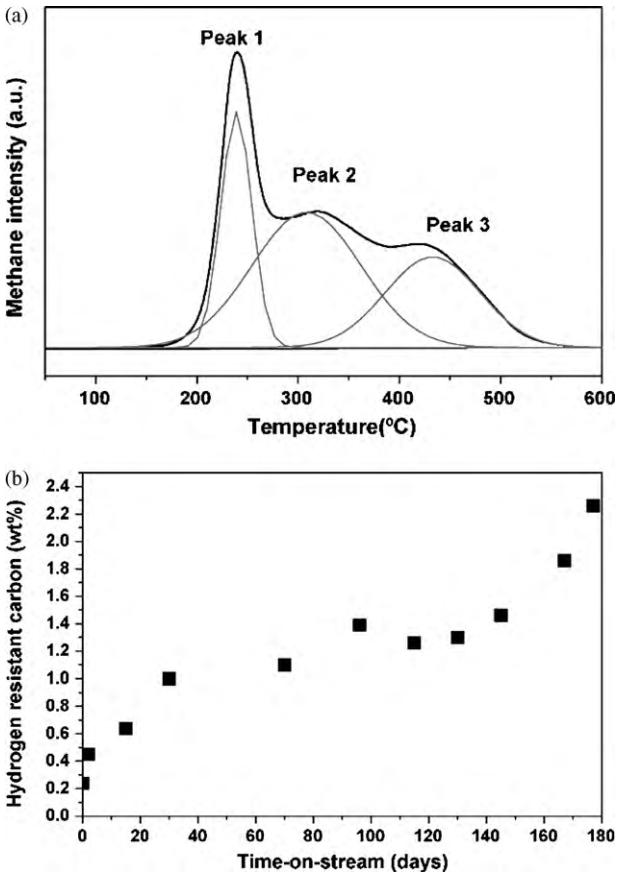

Fig. 6. (a) Peak deconvolution of a methane profile for TPH of a wax-extracted $Co/Pt/Al_2O_3$ catalysts from the FTS run in the slurry bubble column. (b) Carbon amounts obtained from TPO experiments following TPH which represents carbon resistant to hydrogen at 350 °C.
Adapted from reference [61].

unloaded periodically from the reactor and treated under inert conditions. The wax was removed by tetrahydrofuran extraction before the samples were characterized by temperature programmed techniques, EF-TEM and HS-LEIS. The study was based on temperature programmed hydrogenation followed by temperature programmed oxidation experiments. The correlation of temperature programmed hydrogenation (TPH) data with reported values of the hydrogenation resistance of hydrocarbon species suggest that high molecular weight carbon species, polymeric in nature and amorphous in structure, were accumulated during the run (peak 3 in Fig. 6a). Subsequent temperature programmed oxidation (TPO) gave a quantitative approximation of the amount of hydrogen resistant carbon accumulating on the surface (Fig. 6b). The nature of the carbon species was confirmed by high resolution-transmission electron microscopy (HR-TEM) and carbon mapping using EF-TEM images gave the topography of polymeric carbon. It appears that the carbon species are located both on cobalt and on the alumina support. The authors believe that the carbon is nucleated on the cobalt sites and then migrating to the support. It was suggested that the polymeric carbon accumulation was responsible for the long-term deactivation of FT catalyst [61]. Catalyst deactivation due to carbon deposition on cobalt crystallites has also been proposed by BP based on results from laboratory plug flow reactors and a demonstration pilot plant [82].

Several studies have been published dealing with the positive effect noble metals may have on suppressing carbon formation during FTS. Ruthenium addition is considered to retard carbon deposition in addition to increasing the activity, selectivity, dispersion and reducibility. It is known that ruthenium based FTS catalysts

have better resistance to carbon formation compared to other metals [83]. Iglesia et al. have reported that Ru addition acts as an inhibitor for carbon formation [84]. A Ru-promoted and an unpromoted Co/TiO_2 catalyst were used in a fixed-bed reactor ($\geq$200 °C, 20 bar, $H_2/CO = 2.05$). The promoted catalyst showed no evidence of carbon formation even at 500 °C, whereas the unpromoted catalyst formed carbon filaments which encapsulated the cobalt particles at lower temperatures (400 °C). The importance of calcination during catalyst preparation is emphasized for obtaining contact between the cobalt metal and the promoter, apparently essential for the promotional effect. In addition, model catalysts were used and studied with XPS. It appears that the deactivation by carbon deposition might be the reason of initial catalyst deactivation, since both catalysts (Co and Co-Ru) exhibited similar long-term deactivation characteristics.

It is known that catalyst deactivation may be a result of filamentous carbon formation including carbon nanofibre structures, in particular at high temperatures [85]. These stable carbon species can be formed in environments containing carbon monoxide or a gaseous hydrocarbon. Cobalt metal is known to catalyse this growth [86]. Thus, it is expected that cobalt based FT catalysts will exhibit similar behaviour at given conditions. Studies of a Pt promoted cobalt catalyst supported on Al_2O_3 and a NaY zeolite [87] have shown the formation of carbon nanotubes, carbides and amorphous carbon. The catalyst was exposed to CO atmosphere at 750 °C and 10 bar and subsequently characterized by several methods including TEM. It was proposed that CO disproportionation is led to carbon nanotube formation that encapsulated only the cobalt particle through the formation of a Co_xC metastable carbide which acted as an intermediate. It is evident that those conditions are not FT relevant, but the authors suggested that the mechanism of carbon growth may be linked to H_2-deficient FT processes. Similarly, Jun and co-workers detected filamentous carbon formation at milder conditions (220–240 °C, 20 bar and $H_2/CO = 2.017$) by using an amorphous aluminium phosphate ($AlPO_4$)-supported cobalt catalysts [88]. No sign of filamentous carbon formation was observed on a similar Ru-promoted $Co/AlPO_4$ and Co/Al_2O_3 catalysts. The authors correlated the filamentous carbon formation with the higher deactivation rates for the unpromoted $Co/AlPO_4$.

It is evident from several observations that ruthenium addition leads to less carbon formation. Apart from noble metals, alkali metals may also have a retarding effect on carbon formation. Somorjai and Lahtinen [89] investigated the effect of potassium addition to model catalysts. Polycrystalline cobalt foils were prepared and potassium addition investigated by subjecting the catalysts to synthesis gas atmosphere at >250 °C, 1.01 bar and $H_2/CO = 3$ followed by subsequent characterization using AES. Despite the shift in the catalysts selectivity towards C_{3+} hydrocarbons, potassium promotion led to increased resistance towards graphite formation.

Recently boron was proposed as an additive for the minimization of carbon deposition [90]. DFT calculations coupled with experimental results from FTS showed that the addition of 0.5 wt% B enhanced catalysts stability by a factor of 6. Computational calculations suggested that boron reduces graphene nucleation and initiation of a clock reconstruction (see Section 2.3.3).

Apart from the use of promoters, different solutions have been applied for suppressing fouling by carbon deposits. Supercritical fluids have been proposed as alternative solvents for use in the FT reactors. Supercritical media are showing exceptional mass transfer characteristics and it is believed that they will not allow heavy hydrocarbons to accumulate and deactivate the catalyst [91]. In addition, multifunctional catalysts having a cracking ability have been employed in FTS [92,93]. The catalysts are encapsulated in an H-β-zeolite shell which does not allow heavy hydrocarbons to build up. As a result the high molecular weigh products are passing through a process including hydrocracking and isomerization to isoparaffins. These catalysts have showed increased stability. However, the selectivity of such systems changes dramatically favouring lighter hydrocarbons and are hence suitable when products in the gasoline range are desired.

Studies on model catalysts have also been carried out by Geerlings and co-workers [94,95]. They studied the behaviour of Co single crystals in FTS at temperatures between 220 and 300 °C, 1 bar total pressure and $H_2/CO = 2$. The investigation covered several different cobalt surfaces including (0 0 0 1), (1 1 $\bar{2}$ 0) and (1 0 $\bar{1}$ 2) using electron energy loss (EELS) and AES spectroscopies. Both techniques indicated the existence of CO and CH_x surface species after the reaction. In addition, spectroscopic data showed a higher selectivity towards long chain hydrocarbons ($>C_3$) in the zigzag grooved (1 1 $\bar{2}$ 0) surface, whereas the other surfaces were covered mainly with CO and light hydrocarbons. The activity of the stepped sites in CO dissociation was higher than for the flat surface. The authors described the reaction as self-poisoning, due to the fact that carbon may poison the catalytically active sites. The results suggested that the balance between carbon deposition via CO dissociation and carbon removal via hydrogenation is destroyed when carbon atoms are strongly bonded to the step sites. The strongly chemisorbed carbon cannot be efficiently hydrogenated under FT conditions and is thus poisoning the surface. Subsequently, it builds up to form other carbon species which deactivate the catalyst. It should be noted that the pressure gap between ultra high vacuum (UHV) conditions and realistic FT conditions may significantly change the behaviour of the catalyst.

In addition to model studies, the effect of carbon in FTS has attracted interest from computational chemistry [96,98]. Zonnevylle et al. applied preliminary calculations using a Hartree–Fock–Slater linear combination of atomic orbitals (HFS-LCAO) on a cobalt cluster consisting of nine atoms [96]. The calculations showed that in such a cluster and under specific conditions subsurface carbon formation may prevail at the expense of surface carbidic species. It appeared that the energy barrier of subsurface carbon formation is relatively high in a fixed lattice. However, the calculations showed that the effect of surface stretching (1%) and relaxation combined with oxygen coadsorption can decrease the barrier by as much as 90%, making subsurface carbon formation feasible. In addition, it is noted that the existence of a subsurface carbon configuration is expected to lead to an electronic modification of the surface and subsequent inhibition of CO adsorption and the reaction.

A recent study incorporated the use of computational techniques for the investigation of graphitic carbon formation on a flat *fcc*-Co (1 1 1) surface [97,98]. Density functional theory (DFT) calculations were used to probe the most energetically favourable routes for graphitic carbon formation. It was found that the initially adsorbed carbon, which was a result of carbon monoxide dissociation, was highly mobile especially at low coverage. These atomic carbon species were building up on the surface in order to create linear and branched carbon structures, with the linear ones being energetically favourable. Subsequently high coverage of those species will give rise to the formation of aromatic clusters by linkage. Further growth from atomic carbon addition or from C–C coupling resulted in the formation of more stable graphene structures. In order to facilitate the interaction of graphene with the cobalt surface, DFT calculations were supplemented by partial DOS (density of states) and Bader charge analysis calculations. Calculations also indicated that graphene is chemisorbed on the cobalt surface and that the heat of adsorption is equal to −4 kJ/mol carbon. Although the normalized value per cobalt atom is low, it is significant for long graphene clusters. Accordingly, extended structures will either slide away from the surface and possibly end up on the support or even be immobilized due to the prosthetic chemisorp-

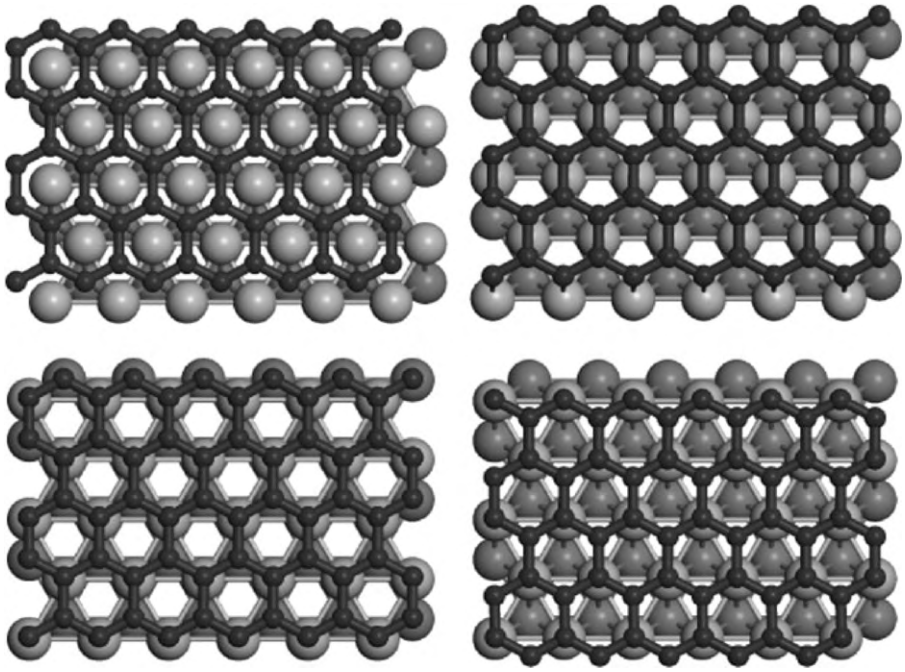

Fig. 7. Adsorption sites for graphene on *fcc*-Co (1 1 1) at ring-top, ring-bridge, ring-*fcc* and ring-*hcp* sites (top layer Co atoms: light gray; second layer Co atoms: dark gray; carbon atoms: black). A $p(1 \times 1)$ unit cell was used for all calculations. Tests with larger $p(2 \times 2)$ unit cells gave similar results.
Adapted from reference [98].

tion. Different configurations of the system grapheme-metal are presented in Fig. 7.

2.3.3. Carbon induced surface reconstruction

Cobalt surfaces reconstruct during FTS and reconstruction could alter catalyst behaviour. Changes in the surface configuration during FTS may lead to alternation of the nature of active sites and hence to activity variations. Reconstruction may also render the surface more sensitive to events which may deactivate the catalyst. These changes may be induced from adsorbed species, e.g. CO, O, N, S or other molecules including carbon containing intermediates and products [99]. Thus, an indirect contribution of surface reconstruction to activity loss should not be neglected. The detection of these phenomena needs sophisticated instrumentation and as a dynamic phenomenon, it may not be visible by *ex situ* techniques. Most studies are based either on probe microscopic examinations of model compounds or computational approaches.

The contribution from studies on model surfaces in FTS is significant [100]. de Groot and Wilson [101] reported the restructuring of a model flat Co (0 0 0 1) surface to triangular shaped cobalt islands when subjected to CO hydrogenation conditions (Fig. 8) (250 °C, 4 bar and constant flow 1 ml/min of H_2/CO = 2). The existence of surface restructuring phenomena under the influence of CO was further confirmed by polarization modulation-reflection absorption infrared spectroscopy (PM-RAIRS) experiments in similar model catalysts [102,103].

Scanning tunneling microscopy (STM) was used at UHV conditions on a clean metal surface. The proposed mechanism consists of an etch-regrowth process which is triggered by the mobility of the formed sub-carbonyl adspecies, i.e. $Co(CO)_x$ (x = 1–4). This mechanism seems to be favourable since it does not require a net loss of cobalt atoms via the gas phase and is further strengthened by the fact that several inductively coupled plasma (ICP) analyses of spent catalysts suggested negligible cobalt loss during FTS [41,42,50,51]. However, industrial scale extended runs may result in significant loss of the catalytically active component [5].

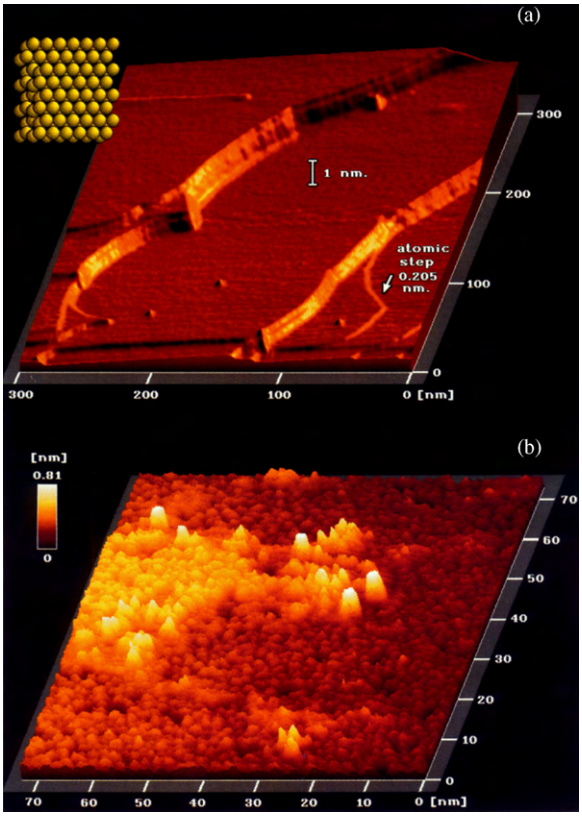

Fig. 8. (a) STM image of the clean Co (0 0 0 1) surface (prior to reaction) showing atomically flat terraces 150 nm (ca. 600 atoms) in width (tunneling current I_t = 2 nA, sample bias V = 0.05 V). The smallest step visible is monatomic in height, 0.205 nm being the expected single atom step height on Co (0 0 0 1). (b) STM image of the Co (0 0 0 1) surface after 1 h exposure to high-pressure CO hydrogenation conditions (I_t = 0.5 nA, V = 0.5 V). Inset: hard-sphere model of the bulk-terminated Co (0 0 0 1) surface.
Adapted from reference [101].

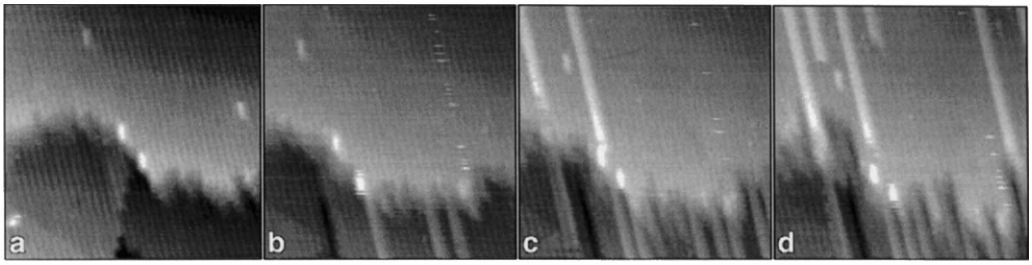

Fig. 9. Sequence of 200 × 200 Å STM images showing the formation of the (1 × 2) added row structure. (a) Clean surface with a monoatomic step. (b) 0.6 L CO. (c) 1.0 L CO. (d) Evacuation for 8 min 30 s after 1.0 L CO exposure.
Adapted from reference [105].

Venvik et al. studied the effect of carbon monoxide adsorption on $(1\,1\,\bar{2}\,0)$ and $(1\,0\,\bar{1}\,2)$ cobalt surfaces at room temperature using STM [104,105]. The atomic scale images of the crystals showed that adsorption induced restructuring took place on both surfaces. In particular, molecular adsorption of carbon monoxide on a Co $(1\,1\,\bar{2}\,0)$ surface induced migration of Co atoms along the $(0\,0\,0\,1)$ direction. The diffusion of the cobalt on the surface was found to be anisotropic and atoms migrated over distances up to 300 Å. In agreement with previous proposals the mobile species was suggested to be carbonyl-like species, without the exclusion of single atom or cluster diffusion. Similarly on a Co $(1\,0\,\bar{1}\,2)$ surface and upon CO adsorption added rows were found to nucleate and grow from the step edges of the surface. Co atoms seem to be released from the step edges to form the added rows (Fig. 9).

Since direct detection of surface reconstruction of industrial type catalysts is still relatively rare [106], number of studies are indirectly related to surface restructuring. Schulz et al. suggested that there is an incubation period from the start of the reaction until the catalyst reach an FT active structure [107,108]. This active structure, which in the article is referred to as the "true catalyst", is formed and stabilized only under FT conditions. In order to link the state of the surface with the reaction a detailed product analysis was performed. The theory relies on the fact that changes in the catalytically active species will be reflected in the product distribution. Three SiO_2 supported and promoted cobalt catalysts were prepared and used in a laboratory reactor at 463 K, 5 bar and $H_2/CO = 1.9$. The catalysts were promoted with Re, Pt and Ir, respectively. The resulting plot of the CO conversion with time on stream in logarithmic scale reveals three different kinetic regimes (not presented here). Further data analysis of the product distribution together with the fact that the activity increases about three times after some days on stream, led to the hypothesis that slow restructuring of the cobalt crystallite surface occurs and leads to the creation of a new rough surface with increased area. This rough surface consists of characteristic sites with different coordination numbers, which are described as peaks, holes and planes. It was proposed that these sites are responsible for different FT reactions such as chain growth, CO dissociation and hydrogenation, respectively. Ultimately, it was suggested that this reconstruction results in a segregation (roughening) of the cobalt surface, induced by the strong CO chemisorption. However, reconstruction of cobalt surfaces is related to the activation period of FTS. The only correlation that has been done with catalyst deactivation is related to the on-plane sites, of medium coordination, which may be poisoned (reversibly) by adsorbed CO and methyl species. In addition, it was proposed that sintering of the metal crystallites will be compensated for by the strong chemisorption of CO which will stabilize a segregated surface.

Bezemer et al. investigated the influence of cobalt particle size on FTS. In accordance with the above described studies they reported experimental indications of cobalt surface reconstruction [109]. EXAFS data taken from spent carbon nanofibre supported cobalt catalysts, with crystallites in the range of 2.6–27 nm, revealed a decrease in the first shell Co–Co coordination number of about 6–7% after exposure to synthesis gas. This change in the coordination number indicates a reconstruction of the cobalt crystallites during FT synthesis. It is worth to mention that the authors did not detect any other phenomena that may lead to catalyst deactivation, i.e. sintering, re-oxidation or carbidization.

Along with other simulation studies on the cobalt crystallite behaviour at reaction atmospheres, density functional theory has been employed in order to resolve restructuring phenomena. The importance of carbon adsorption is addressed. Ge and Neurock have performed periodic DFT calculations on adsorption and activation of CO on several cobalt surfaces [110]. Models of flat Co $(0\,0\,0\,1)$, corrugated Co $(1\,1\,\bar{2}\,0)$, and stepped Co $(1\,0\,\bar{1}\,2)$ and Co $(1\,1\,\bar{2}\,4)$ surfaces were compared. Simulation of various adsorption configurations on these surfaces and the least energetically demanding configuration was determined. It was found that significant surface reconstruction was induced by C adsorption in the Co $(1\,0\,\bar{1}\,2)$ stepped surface. In particular the adsorption of the C atom at the hollow site pushes the Co rows apart in the $(0\,1\,0)$ direction by 0.2 Å. A more recent DFT study emphasizing on $(1\,1\,1)$ and $(1\,0\,0)$ *fcc*-cobalt surfaces has been performed by Ciobîcă et al. [111]. From the several simulated adsorbate candidates, i.e. O, CO, CH_2, CH and C, it was proposed that only carbon is able to induce surface reconstruction on the two surfaces. Calculations also show that a *fcc*-Co $(1\,1\,1)$ surface, with 50% adsorbed carbon, will reconstruct to a *fcc*-Co $(1\,0\,0)$ surface which subsequently will undergo a clock type reconstruction, while *fcc*-Co $(1\,0\,0)$ will give a clock type reconstruction in presence of carbon. This surface rearrangement will increase the number of carbon atoms neighbouring cobalt atoms from four to five and thus create a more stable configuration which will eventually poison the surface or assist in the formation of stable carbon species (see Section 2.3.2).

It should be mentioned, that due to the complexity of the FT environment theoretical studies are subjected to several assumptions. Thus, the influence of different adsorbed species (e.g. H_2) is not always taken into consideration.

2.4. Re-oxidation

A frequently debated topic in cobalt based FT catalyst deactivation is the possible re-oxidation of cobalt active sites during synthesis and the subsequent formation FT inactive cobalt oxides. This hypothesis arises from the fact that water, the most abundant byproduct of FTS, is an oxidizing agent and thus may cause surface oxidation of the cobalt nanoparticles. Water, which is present in the form of steam under normal FT conditions, originates from side reactions of surface oxygen and hydroxyl species that are removed from the surface via hydrogenation [112]. The effect of water in FTS is well documented and described from different perspectives in recent reviews [2,113,114].

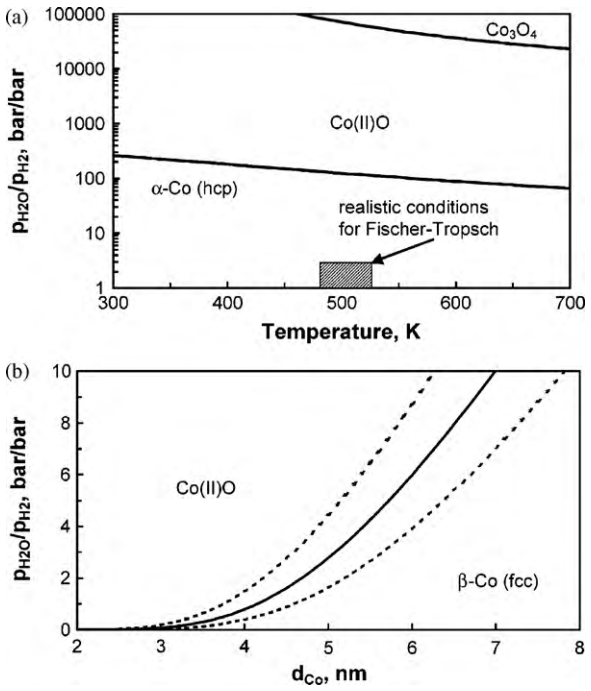

Fig. 10. (a) Stability diagram of bulk cobalt metal and various cobalt oxide phases as a function of temperature and ratio of partial pressure of water to partial pressure of hydrogen. (b) Stability region of spherical β-Co (*fcc*) and Co(II)O crystals in H_2O/H_2 atmospheres at 220 °C as a function of the diameter of a spherical metal Co crystallite (dotted line $\gamma_{\beta\text{-}Co} \pm 15\%$).
Adapted from reference [115].

The most commonly applied technique for studying the re-oxidation is the co-feeding of water during low-conversion FTS activity measurements. This is believed to resemble high conversion FTS experiments in slurry reactors. However, extended runs and low space velocity runs have also been performed. The spent catalysts, subjected to such conditions could be analyzed for the detection of re-oxidation of active species with TPR, XPS, Mössbauer Emission Spectroscopy (MES) and XANES. XANES appears to be the most successful technique, since it can give quantitative results on the degree of reduction (DOR) and can be applied without removing FT waxes that are covering the surface of the catalyst. Thus, the catalyst is protected from air exposure. However, for XANES experiments synchrotron radiation is needed.

It is known that the bulk oxidation of metallic cobalt is not feasible under realistic Fischer–Tropsch synthesis conditions [11,115] (Fig. 10a). However, it is expected that the behaviour of cobalt nanoparticles may deviate from the properties of the bulk cobalt at FT conditions (Fig. 10b). Thermodynamic calculations have shown that spherical cobalt crystallites less than 4.4 nm in diameter may oxidize in steam–hydrogen environments ($P_{H_2O}/P_{H_2} < 1.5$, corresponding to 75% CO conversion and 220 °C) commonly encountered in FTS [115]. The calculations were based on the surface energies of cobalt crystallites that are different in size (<100 nm), morphology (e.g. spherical shape) and the initial crystal phase (e.g. β-Co (*fcc*)). Calculations have also shown that formation of an oxide shell surrounding a metallic core is thermodynamically unstable. However, the contribution of support interaction and surface reconstruction at FTS conditions was not taken into consideration.

Numerous studies have still pointed to the possible existence of surface re-oxidation in the complicated/crowded FTS environment. The relation between external addition of steam in order to simulate high conversions and the resulting FTS activity and selectivity has been studied by several groups. Schanke et al. [116,117] studied a rhenium promoted and an unpromoted Co/γ-Al_2O_3 catalyst. The catalysts were subjected to several different tests including co-feeding of steam or by using pure H_2O/H_2. Results from TPR and gravimetric studies indicated re-oxidation to a small extent, depending on the conditions. It was proposed that surface oxidation and in particular oxidation of highly dispersed fractions of the cobalt could take place. Steady state isotopic transient kinetic analysis (SSITKA) performed at methanation conditions (CO conversion <15%, 210 °C, 1.85 bar and $H_2/CO = 10$) using the same catalyst as above [118] showed an increased olefin selectivity and unchanged intrinsic catalytic activity with respect to the methane formation after steam addition.

Further experimental studies also concluded loss of active sites [119,120]. These experiments were carried out on 17 wt% Co/γ-Al_2O_3 and 1 wt% Re-17 wt% Co/γ-Al_2O_3 catalysts at 210 °C and 13 bar. The externally added steam was kept at the ratio of $H_2O/H_2 = 1.5$, simulating the environment of approximately 75% CO conversion. In agreement with previous observations the promoted catalyst appeared to deactivate faster. This deactivation was more pronounced at high steam partial pressures. Temperature programmed desorption (TPD) results indicated a significant loss in the cobalt surface area which is in line with the previous reports. TPR and gravimetric studies showed indications of re-oxidation in the presence of steam.

Catalysts on different supports with various pore size distributions have been evaluated [121–125]. Experiments with unpromoted and Re-promoted Co catalysts on different supports (i.e. γ-Al_2O_3, SiO_2, TiO_2) with various pore size distributions have shown that the observed deactivation depends on the support. For Co supported on γ-Al_2O_3, addition of steam in the feed resulted in loss of activity with time on stream and most pronounced for the Re-promoted catalyst. As shown in Fig. 11, different behaviour was observed of Co supported on SiO_2 and TiO_2. Additionally, it was found that small amounts of water (H_2O/H_2) = 0.4 on TiO_2 and SiO_2 supported catalyst may benefit the activity. However, the effect of steam has to be discussed with respect to crystallite size, support interaction and catalysts structural characteristics (e.g. pore size). Alumina supported catalysts were further studied and the importance of the pore characteristics were evaluated [125]. It was found that small pores yield lower reaction rates, while larger pores give higher rates. Irrespective of the support, it is observed that steam addition has a positive effect on the C_{5+} selectivity. Promoted catalysts deactivated more rapidly than their unpromoted counterparts.

One of the earliest *in situ* XAS investigations on FT catalysts was done on K-promoted and unpromoted cobalt catalysts supported on SiO_2 and Al_2O_3 with only 9 and 4.4 wt% Co, respectively [126]. The *in situ* cell was similar to the one designed by Lytle et al. [127]. Experiments were performed at ambient pressure and 190–200 °C, while the H_2/CO ratio was equal to 3. External water addition was also applied. Both K-edges of potassium and cobalt were investigated. Results for the silica-supported catalyst are suggested that re-oxidation of the unpromoted catalyst took place when water vapour was externally added to the system, while the promoted maintained its degree of reduction. On the contrary the promoted alumina supported catalyst was apparently converted to a mixture of Co_3O_4 and CoO at reaction conditions at 200 °C. The unpromoted counterpart did not change significantly.

Mössbauer emission spectroscopy has also been employed in combination with thermogravimetric analysis for the detection of changes in the oxidation state of cobalt [128,129]. Application of the MES technique is challenging, since the catalyst has to contain a fraction of the radioactive isotope ^{57}Co. The catalysts were supported on alumina and promoted by platinum. However, the doped catalyst for MES characterization was prepared in a slightly different manner. The catalyst was subjected to model gaseous mixtures of H_2, H_2O and Ar. FTS runs were performed in a labo-

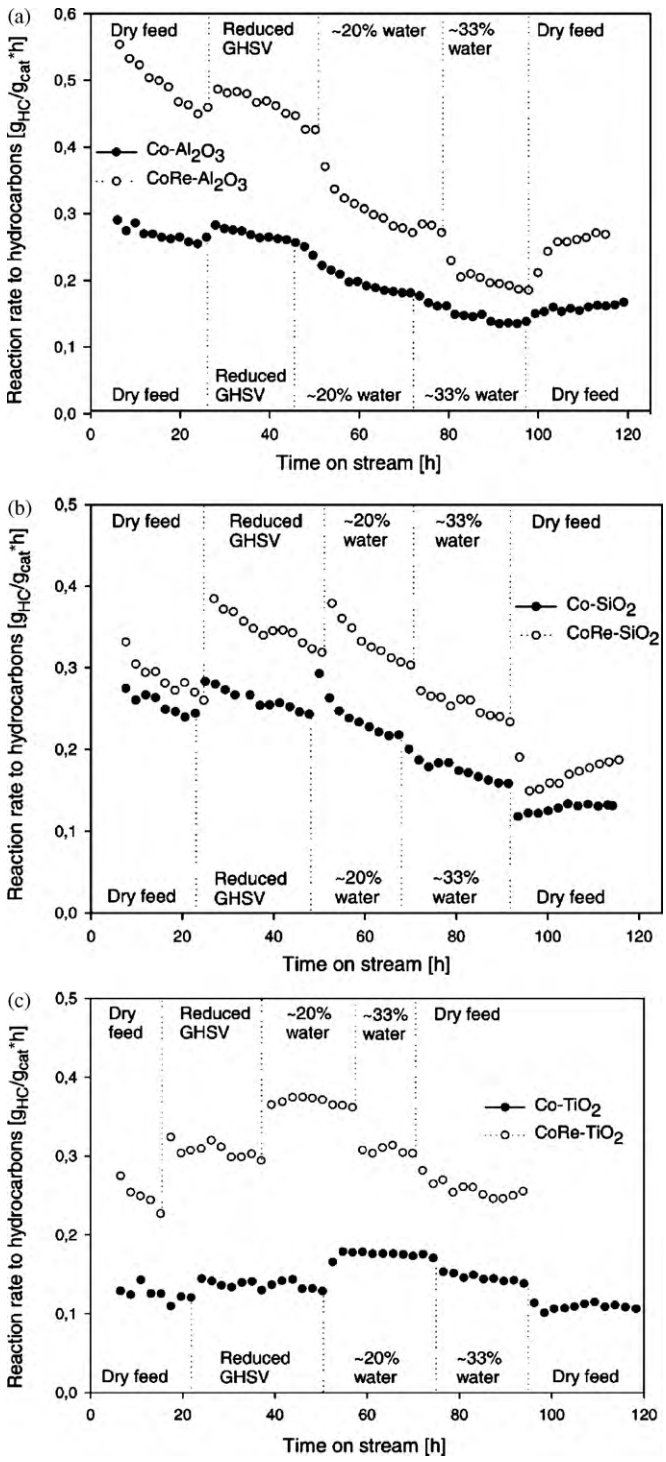

Fig. 11. Observed reaction rate for formation of hydrocarbons as a function of time on stream 5 h after start-up for Co (●) and CoRe (○) catalysts supported on Al_2O_3 (A), SiO_2 (B), and TiO_2 (C). $H_2/CO = 2.1$, $P_{Total} = 20$ bar, $T = 210\,^{\circ}C$. Adapted from reference [124].

ratory CSTR (220 °C, 20 bar, and 50–70% synthesis gas conversion levels). Results from the model studies showed that re-oxidation of the catalyst occurred depending on the P_{H_2}/P_{H_2O} ratio which is in contradiction with bulk phase thermodynamics. Formation of both reducible and less reducible cobalt oxide species was observed by MES and was in agreement with the thermogravimetric studies. Data from realistic FTS combined with steam feeding indicated a second cause of deactivation in addition to poisoning. Based on their model studies, the authors did not exclude re-oxidation as a possible deactivation mechanism. Further studies were performed under atmospheric pressure. The group also reported the design of a high-pressure cell. Data obtained from the high-pressure cell are suggesting further reduction of the catalyst with increasing total pressure during treatment with a gas mixture having $P_{H_2}/P_{H_2O} =$ 1.0 at 150 °C and pressures up to 10 bar [130]. The importance of reaction conditions on the re-oxidation phenomena should hence be emphasized.

Sasol in cooperation with university research groups has employed advanced characterization techniques like HR-TEM, TPR, XRD, XAS and magnetism in an attempt to further investigate the influence of water and the potential re-oxidation of industrial catalysts. Simultaneously, EXAFS, AFM, XPS and Rutherford backscattering spectrometry (RBS) were used to study model catalysts. Initially, a planar $Co/SiO_2/Si(1\,0\,0)$ model catalyst with cobalt crystallites of 4–5 nm was prepared and subjected to FTS simulated environment ($H_2/H_2O = 1$, $P_{Total} = 0.4$ mbar, and 150–450 °C) [131]. The catalyst was characterized before and after treatment. Near-edge X-ray absorption fine structure (NEXAFS) results from the Co L_{III}-edge showed no indication of re-oxidation at the present conditions. It was proposed that crystallites within this size range did not re-oxidize during FTS. Additionally, spherical Co/SiO_2 model catalysts were prepared having cobalt crystallites with average size of 4, 13 and 28 nm and their behaviour against oxidation was also examined [132]. A strongly oxidizing environment was used (H_2O/He, $P_{H_2O} = 0.04$ bar). The catalysts were subjected to these conditions and showed different behaviour highly depending on crystallite size. The catalyst having small crystallites (i.e. 4 nm) was surprisingly resistant to re-oxidation. Although the catalyst underwent mixtures of H_2O/He at $P_{H_2O} = 0.04$–0.3 bar, it did not show any re-oxidation, which is in contradiction with previous thermodynamic calculations [115]. The observation was attributed to metal–support interactions resulting in crystallite encapsulation by the support. The assumption was supported by TPR and HR-TEM results. Larger crystallites were oxidized in gaseous mixtures of H_2O/He ($P_{H_2O} = 0.04$ bar) reaching a maximum of 30% oxidation at 300 °C. Crystallites around 28 nm showed less than 2% oxidation at the same conditions. The authors emphasized the difficulty of re-oxidation of these models and the strong size dependence.

The next step in this series of studies included XANES characterization of industrial catalysts operated in a slurry bubble column reactor having a capacity of 100-barrel/day at commercial FTS conditions (230 °C, 20 bar, synthesis gas conversion between 50% and 70%) [133]. A 20 wt% Co, 0.05 wt% Pt supported on γ-Al_2O_3 catalyst with average crystallite size of 6 nm was unloaded from the reactor at different times throughout its operation over a period of 140 days. The FTwax protected catalysts were characterized by means of XANES (Fig. 12). Linear combination of the spectra with standards gave a quantitative approach of the changes in the degree of reduction during operation and the fraction of metallic cobalt was found to increase from 50% to 88% (Table 1).

Based on these results it was concluded that re-oxidation can be ruled out as a deactivation mechanism of cobalt crystallites larger than 6 nm supported on alumina at the applied FTS conditions. In order to verify their conclusions the group employed X-ray diffraction and magnetic measurements [113]. The results from magnetic measurements were in line with XANES, showing from the saturation magnetisation the degree of reduction or the amount of cobalt metal. X-ray diffraction results verified the observations by demonstrating the disappearance of the CoO peaks after 3 days on stream. The authors proposed that re-oxidation is not a significant deactivation mechanism for alumina supported cobalt catalysts at industrially relevant FT synthesis conditions. Potential deactivation by oxidation can be prevented by the correct combination of partial pressures of hydrogen and water (P_{H_2}/P_{H_2O}) and the crystallite size

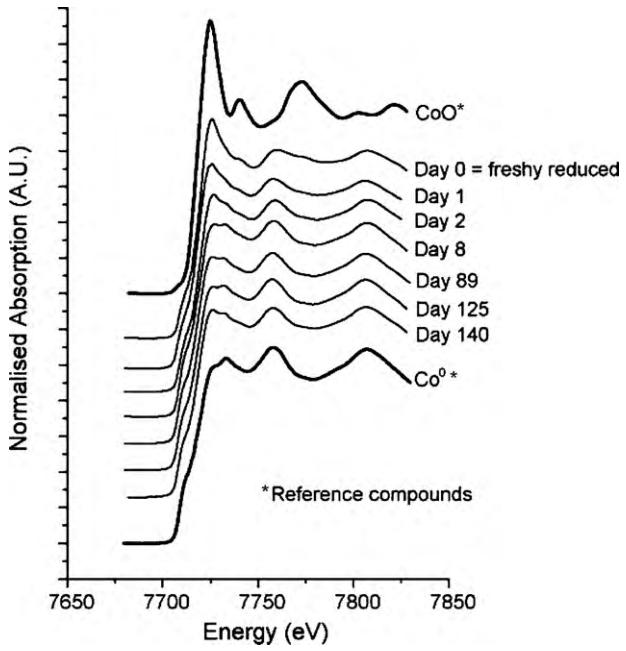

Fig. 12. XANES analysis of a series of spent $Co/Pt/Al_2O_3$ catalyst samples taken from a 100-barrel/day slurry bubble column reactor operated at commercially relevant FTS conditions, i.e. 220 °C, 20 bar, (H_2 + CO) CO conversion between 50% and 70%, feed gas composition of ca. 50 vol.% H_2 and 25 vol.% CO, $P_{H_2O}/P_{H_2} = 1–1.5$, $P_{H_2O} = 4–6$ bar. Adapted from reference [133].

of cobalt. It should be noted that the low starting DOR suggests a partially reduced fresh catalyst. The CoO content in such a catalyst is expected to be high and may influence the interactions between the metal and the support leading to different deactivation behaviour. Recently, Botes [134] reported that the kinetic effect of steam on the overall FT reaction rate is negligible. However, it affects product distribution, mainly by lowering CH_4 selectivity while increasing the selectivity to CO_2. In addition long-term exposures appear to increase the irreversible deactivation.

Iglesia has stated that small crystallites appear to be less active for CO hydrogenation than larger crystals [112]. This was attributed to stronger support interactions, reflected in the incomplete reduction of CoO and even the re-oxidation of Co metal by water formed in the FTS. It has also been suggested that crystallites of 5–6 nm may re-oxidize and deactivate rapidly in the presence of water at typical FTS conditions. A more recent *in situ* infrared spectroscopic study [135] on a 12.7 wt% Co/SiO_2 catalyst (200 °C, 5 bar and $H_2/CO = 2$) suggested that water does not influence the density or structure of adsorbed CO intermediates nor the number of exposed cobalt atoms. However, subjecting the catalyst to a simulated FTS environment (H_2O/H_2 ratio > 0.8 at 200 °C) resulted in surface oxidation and the formation of adsorbed oxygen islands. The islands do not readily react with adsorbed hydrogen at the same rate as isolated adsorbed oxygen species formed by the CO dissociation reactions.

Table 1
Quantification of XANES analyses of a series of spent $Co/Pt/Al_2O_3$ catalysts taken from a 100-barrel/day slurry bubble column reactor operated at commercially relevant FTS conditions using a linear combination of reference compounds.

Sample	Co^0 (%)	CoO[a] (%)
Freshly reduced	53[b]	47
Day 1	69	31
Day 2	80	20
Day 8	85	15
Day 89	88	12
Day 125	89	11
Day 140	87	13

Adapted from reference [128].
Error = ±2–3%.
[a] The following does not rule out any minor $CoAl_2O_4$, which is difficult to differentiate with XANES using the current data and is most likely present at the interface of the cobalt particles with the support.
[b] Although on the low side, the degree of reduction is close to that obtained from gravimetry, i.e. 63%.

Kiss et al. studied FTS performance of silica-supported cobalt catalysts under hydrothermal FT conditions [39]. The catalysts were subjected either to high CO conversion or steam co-feeding in order to simulate hydrothermal conditions. Catalyst tests were performed in both fixed-bed and slurry autoclave reactors (220 °C, 20 bar, $H_2/CO = 2.1$). TEM-EDS, TGA and XRD techniques were employed for catalyst characterization at different stages. For overcoming the problems facing the characterization, a special reactor assembly was developed allowing hydrogen treatments and inert transfer of the sample [136]. It was found that high conversions (>90%) led to the formation of needle-like crystalline cobalt–silica mixed oxides. This phase transformation believed to be the main cause of deactivation of silica-supported cobalt catalysts at high steam partial pressures. The metal–support compound appeared to be well defined having 1 nm lattice space and atomic ratio Co/Si equal to 1.2/1. Steam treatment of the fresh catalyst led to creation of a similar phase in terms of morphology and composition, supporting the idea that the phenomenon was water induced. Hydrogen treated spent catalyst (at mild conditions) was characterized by TEM and a crystallite size distribution was obtained. The change of crystallite size of the freshly reduced and spent catalyst suggested that sintering is also a deactivation route. A regeneration procedure was presented and involved a high temperature (≥400 °C) hydrogen reduction at 1.2 MPa. During the regeneration procedure the cobalt–support mixed oxide decomposed and metallic cobalt crystallites were formed having a bimodal size distribution. It appears that re-oxidation of cobalt is the intermediate of a process which assists to sintering and formation of inactive mixed oxides with the support.

Recently an investigation of the initial deactivation mechanisms of FTS was presented supporting previous observations [29]. EF-TEM, XPS, EXAFS, TGA, Secondary ion mass spectrometry (SIMS) and chemisorption techniques were applied on catalysts operated at 5–35 bar and 200–230 °C. Experimental observations suggest that re-oxidation occurs during FTS and increases the mobility of cobalt crystallites, which are wetting the surface, facilitating sintering or leading to the formation of cobalt–support mixed compounds. The effect is highly related to the crystallite size and conversion level. In addition the importance of the mean crystallite distance is addressed. Regenerated catalysts through a ROR cycle showed higher sensitivity to sintering due to its bimodal size distribution and mean crystallite distance, thus deactivated faster.

Davis and coworkers have performed a comprehensive study on the kinetic effects of water during FTS and the possibility of re-oxidation of cobalt crystallites [137–141]. Li et al. studied the effect of water for different supports [142–145]. Promoted or unpromoted cobalt catalysts with 10–15 wt% Co, supported on SiO_2, Al_2O_3 and TiO_2 were tested in a continuously stirred tank reactor (210–230 °C, 20.2–29.3 bar, 750 rpm and a H_2/CO ratio of 2). The high steam partial pressures were controlled either by varying the space velocity (1–8 NL/h/gcat) or by externally adding steam in the feed. In particular, the 0.5 wt% Pt-15 wt% Co/Al_2O_3 catalyst exhibited a slight decrease in the conversion when small amounts of steam were added [142]. This effect was reversible. Increasing the amount of water ($P_{H_2O}/P_{CO} = 1$) in the feed resulted in a permanent deactivation of the catalyst. The CO_2 selectivity increased with the CO conversion. This was taken as an indication of an increasing extent of the water–gas shift reaction from higher water partial pressures, probably due to transformations of cobalt to oxide forms (oxides or mixed metal–support compounds). Similar results

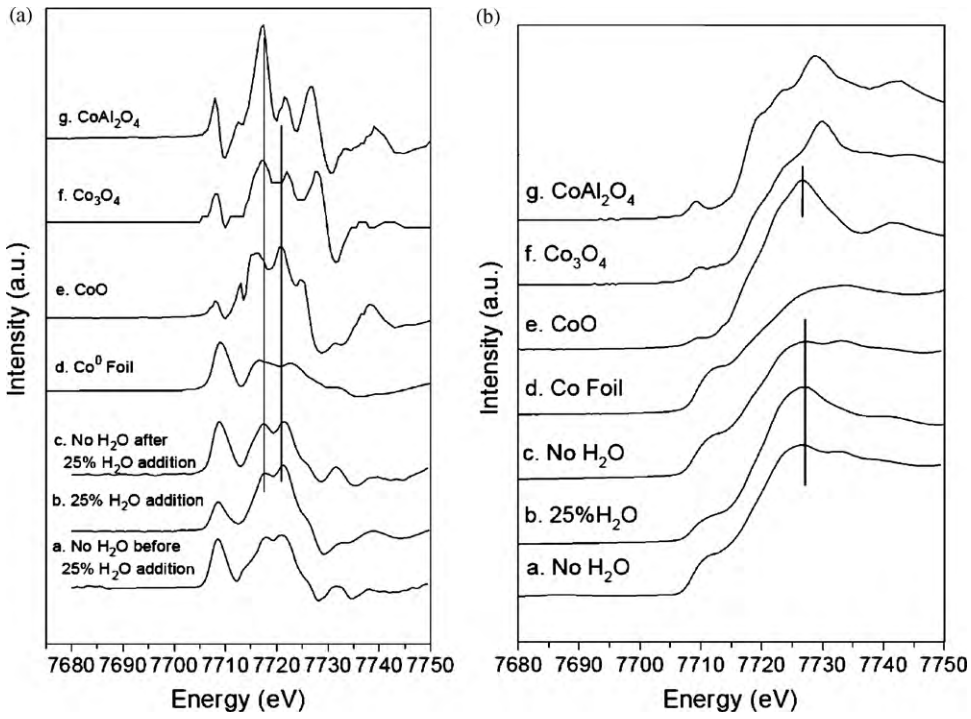

Fig. 13. (A) XANES derivative spectra. Effect of water on 25% Co/Al_2O_3 catalyst moving from bottom to top: (a) after stabilization in the reactor before addition of 25% H_2O; (b) after deactivation in the reactor under 25% H_2O; (c) after recovery period when water was switched off. References are also provided for (d) Co^0 foil; (e) CoO; (f) Co_3O_4; and (g) $CoAl_2O_4$. (B) Normalized XANES spectra moving from bottom to top (a) after stabilization in the reactor prior to addition of 25% H_2O; (b) deactivation in the reactor under 25% H_2O; and (c) after recovery after water was switched off. Inert balancing gas was used and sequentially replaced by water to maintain a constant partial pressure of reactants. References are also provided for (d) Co^0 foil; (e) CoO; (f) Co_3O_4; and (g) $CoAl_2O_4$.
Adapted from reference [148].

were obtained on a 0.2 wt% Ru-10 wt% Co/TiO_2 catalyst [143] where steam addition at low space velocities (2 NL/h/gcat) decreased the CO conversion in a reversible manner, while at higher conversions (1 NL/h/gcat) the deactivation was irreversible. CO_2 selectivity was increased by water addition as well. The unpromoted silica-supported catalyst (12.4 wt% Co/SiO_2) showed different behaviour upon steam addition. It was found that relatively small amounts of H_2O in the range of 5–25 vol.% increased the CO conversion, with the catalyst displaying a high stability throughout the study. However, continuous addition of larger amounts of H_2O led to severe catalyst deactivation. The authors suggested that the difference in behaviour of the silica-supported catalyst may be due to different crystallite sizes (5.6, 8.5 and 13.2 nm on alumina, titania and silica, respectively).

In a later study concerning comparison of results on different supports it was suggested that the formation of a cobalt formate-like species may be a potential explanation for catalyst deactivation, or even the formation of mixed cobalt–support compounds [145]. Particularly for alumina the possibility of support restructuring during reaction at high steam levels (i.e. boehmite formation) was addressed. The role of promoter should be considered as well. Zhang et al. compared the deactivation rates of CO and CO_2 hydrogenations on Pt promoted Co/Al_2O_3 catalyst [146]. For CO_2 hydrogenation the rate of deactivation was not as rapid, despite the higher steam partial pressures. This suggests that assistance of CO is vital in the deactivation process via re-oxidation and that the H_2O/CO partial pressure ratio is more substantial than the H_2O/H_2 ratio. Therefore, it is concluded that the deactivation pathway should involve H_2O and CO, which may synergistically form intermediates that cause the oxidation or crystal growth of cobalt clusters.

X-ray absorption spectroscopy (EXAFS and XANES) has been employed in order to detect a wide range of deactivation mechanisms. Different alumina supported cobalt catalysts were prepared either with promoter addition (i.e. Ru, Re and Pt) or without. The catalysts were tested in a CSTR for FTS activity and subsequently characterized. The ruthenium promoted catalyst was subjected to FTS conditions ($H_2/CO = 2.0$, 220 °C, 20 bar, 33 SL/h/gcat and 15–20% CO conversion levels) and after reactor shut down it was unloaded and cooled in argon atmosphere [45]. XANES spectra were obtained from the wax protected sample. Pre-edge feature and XANES derivative spectra of the samples indicated an increase in the tetrahedral environment of cobalt clusters (Fig. 13). This suggests that either Co_3O_4 or Co-aluminate was formed during reaction. Safe conclusion could not be drawn from the data since both structures contain tetrahedrally coordinated cobalt and thus similar signals. However, it was proposed that since formation of Co_3O_4 is thermodynamically unfavourable the existence of Co_3O_4 is unlikely. In the above study the difference in the behaviour of promoted and unpromoted catalyst was addressed as well. It appears that the promoted catalyst has higher deactivation rate. Based on this observation and the fact that ruthenium appears to act as a reduction promoter, it was suggested that promoter addition allowed the reduction of small cobalt crystallites which are strongly interacting with the support. The small crystallites are deviating from bulk-like behaviour and may re-oxidize during FTS. This explains the higher initial activity rate for the promoted catalyst and accordingly the faster deactivation rate due to the sensitivity of the small crystallites. Jacobs et al. expanded the study by preparing and testing a 0.5 wt% platinum promoted 15 wt% cobalt catalyst and compared with previously characterized systems [46]. The catalysts were tested in a CSTR (220 °C, 18 bar, 750 rpm, $H_2/CO = 2$ and CO conversion levels of about 40%) and characterized mainly with XANES and XRD. Comparison of XANES derivative spectra with reference materials suggested that either Co_3O_4 or cobalt-aluminate like species were formed, with the latter being the most proba-

ble. Again it was suggested that small cobalt crystallites which are strongly interacting with the support and deviating from the bulk cobalt behaviour, may re-oxidize in the presence of water (Fig. 13).

The same Pt promoted catalyst as described above was also investigated by adding steam to the feed [147]. The catalyst was tested in a CSTR at 20 bar, 210 °C, $H_2/CO = 2$ while the amount of externally added H_2O was calculated to be 15 and 30 vol.%. The catalyst was unloaded from the reactor before and after each treatment. For the low-level steam addition, the results suggested that inhibition by H_2O at such levels is probably kinetic, while higher levels create irreversible effects in the catalyst. XANES and EXAFS data strongly suggested that the reason for this observed deactivation was due to structural changes and in particular formation of oxide species such as mixed cobalt-aluminate compounds. Furthermore, Das et al. also investigated the deactivation behaviour of Co/Al_2O_3 catalysts consisting of small amounts of rhenium [47]. A 0.2 wt% Re-15 wt% Co/Al_2O_3 catalyst was tested at 220 °C, 19.9 bar, space velocity 5 SL/h/gcat and 50% CO conversion and withdrawn from the reactor at different times on stream. In contrast to previously reported results, EXAFS data indicated no re-oxidation. The authors suggested that if re-oxidation occurs, it is either limited to the surface of the cobalt crystallites and hence cannot be detected by EXAFS or it is part of a dynamic oxidation/reduction cycle. In addition, it was proposed that rhenium addition may play a role in suppressing re-oxidation.

Jacobs et al. investigated the impact of crystallite size by preparing and testing catalysts with low and high loading, having crystallite sizes between 5–6 and >10 nm, respectively [148]. In this study special attention was given to the effect of high partial pressures of H_2O. Thus, external addition of steam was again employed. EXAFS and XANES results showed clearly different behaviour for the low (15 wt% Co) and high (25 wt% Co) loaded catalysts. The low loaded catalyst with the small crystallites increased interactions with the support and resulted in an irreversible deactivation after water treatment suggesting that cobalt aluminate-like species were formed. Similar to XANES spectra, EXAFS data revealed a decrease in Co–Co coordination of the highly loaded catalysts suggesting the re-oxidation of cobalt to CoO. The crystallites were re-reduced when the H_2O addition was stopped, and the activity displayed a significant recovery. This was believed to be due to a surface oxidation phenomenon.

Similarly, by using *in situ* XANES on a Pt promoted Co/Al_2O_3 catalyst which was reduced in hydrogen at 400 °C, Khodakov observed re-oxidation of 7 nm cobalt crystallites when they were subjected to a H_2O/Ar mixture at 220 °C [149].

Recent studies also indicate that other oxygen containing species can act as oxidizing (deactivating) agents. For instance, carbon dioxide [150], methanol [151] and ethanol [152] have been suggested as mild oxidizers and may be responsible for cobalt re-oxidation or enhancement of the support compound formation. A number of *in situ* studies have been monitoring oxidation state of cobalt by XAS or XPS during FT reaction and they are not reporting any re-oxidation of cobalt crystallites [109,153–155]. Recently, a combined *in situ* XAS-XRD study performed at 18 bar and 210 °C observed no bulk re-oxidation of the cobalt during the FT activation period. However, high temperature operation resulted in further reduction of the catalyst, as observed by XRD, accompanied by sintering of the crystallites [53].

It should be taken into consideration that re-oxidation is reversible under mild hydrogen reduction regeneration treatments and it is thus expected that the activity will be regained. However, the activity is usually partly recovered after mild hydrogen treatments in high conversion FT runs, suggesting the possible existence of several deactivation mechanisms [121].

2.5. Metal–support solid state reactions

Refractory metal oxides are usually chosen as supports in cobalt based FT catalysts [112] and deactivation of the FT catalysts is observed on all commonly used supports. The selection of support materials relies mainly on their ability to be easily manipulated and provide phases with high surface area, unique metal–support interactions and mechanical strength at a competitive price. These characteristics enhance stability of the catalyst by simultaneously lowering the cost of catalyst preparation. γ-Alumina seems to be the preferred support due to its high resistance to attrition, vital for the use in continuously stirred tank or in slurry bubble column reactors, and the ability of stabilizing cobalt clusters, a characteristic which is connected with the resistance against sintering [49]. However, the relatively strong metal–support interaction leads to the formation of hardly reducible cobalt species [156]. It has been reported that such hardly reducible metal–support compounds may act as anchors and make cobalt crystallites more resistant to sintering. [157].

The formation of mixed metal–support compounds is known to occur already during the preparation of the catalyst. Calcination and reduction [158–163] are the steps with high potential for mixed oxide formation. The metal loading is also a critical parameter in metal–support compound formation. Higher diffusion of cobalt ions into the support lattice has been observed for lower loadings [158,164]. Other parameters such as the pH of the impregnating solution during catalyst preparation may be significant [165]. It has been suggested that promoters, e.g. Re, may play an important role in obstructing the diffusion of cobalt into the support by occupying the defect sites of the alumina where the diffusion takes place [166].

The formation of irreducible Co phases during catalyst pretreatment or under reaction conditions is attributed to the migration/diffusion of cobalt cations (e.g. Co^{2+}, Co^{3+}) into the support framework and/or diffusion of cations of the support towards the surface (e.g. Al^{3+}) [167–169]. It appears to be a surface phenomena lacking long range order. For γ-alumina the effect is particularly intense since the metal–support interactions are strong and the similarity of the crystal structures of Co_3O_4 and γ-alumina enhance the ease of migration during calcination. Arnoldy and Moulijn suggested that diffusion of Co^{2+} may occupy tetrahedral sites of $\gamma\text{-}Al_2O_3$ and lead to the formation of Co^{2+} with many O–Al ligands. Additional exchange of Co^{2+} in Co_3O_4 with Al^{3+} may occur [163]. In accordance with this, results from Raman spectroscopy suggested that the formed cobalt-aluminate is not identical to $CoAl_2O_4$ (spinel), but is probably a surface compound deficient in Co [170]. These results were further supported by XAS studies proposing that during reduction a small fraction of the cobalt content is randomly dispersed over the tetrahedral vacancies of the alumina support resulting in an amorphous dispersed phase rather than the bulk $CoAl_2O_4$ spinel [171]. Typical catalyst pretreatment temperatures are too low to allow formation of the bulk spinel. However, small cluster sizes may deviate significantly from the properties of the bulk and experience this partial transformation at the surface level [172]. It has also been found that water may increase the rate of metal-aluminate formation [168].

Useful techniques in identifying mixed metal–support oxides are Temperature programmed techniques [163], Raman spectroscopy [170,173] and XAS [160,172]. For alumina supported catalysts it has been found that XANES derivative spectra of Co_3O_4 and $CoAl_2O_4$ structures may be used to deconvolute contributions from Co^{2+} and Co^{3+} occupying the tetrahedral and octahedral sites, respectively [174].

Goodwin and co-workers performed a series of studies focusing on the formation of mixed metal–support compounds in the catalyst preparation steps and in simulated reaction conditions. Silica supports were first studied for the formation of mixed

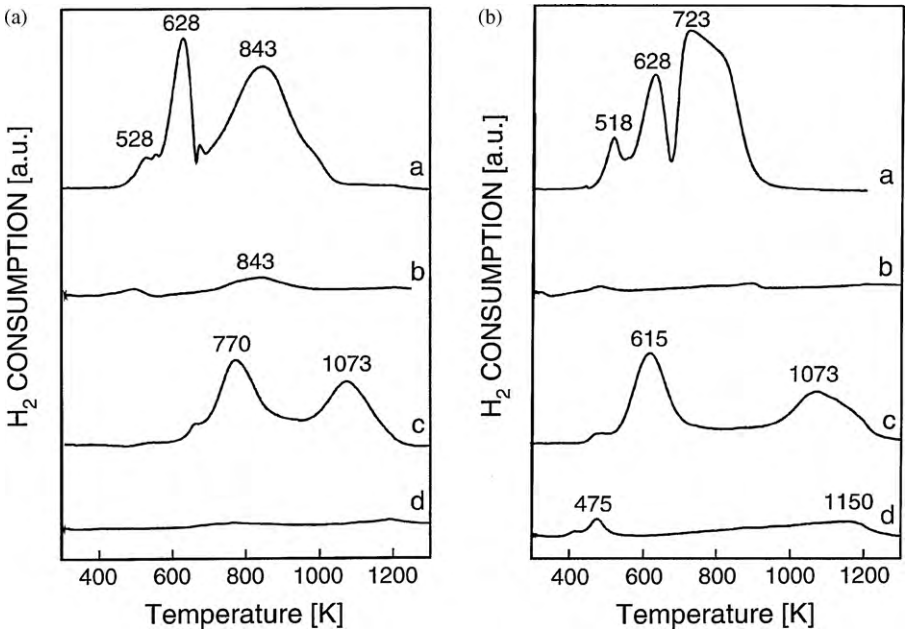

Fig. 14. (A) TPR of Co/Al_2O_3 after calcination (a), reduction (350 °C, 16 h) (b), reduction and exposure to H_2O/He (250 °C, 10 bar, 16 h, 5.5 bar H_2O) (c), and after reduction and exposure to H_2O/H_2 = 10 (250 °C, 10 bar, 16 h, 5.5 bar H_2O) (d). (B) TPR of $CoRe/Al_2O_3$ after calcination (a), reduction (350 °C, 16 h) (b), reduction and exposure to H_2O/He (250 °C, 10 bar, 16 h, 5.5 bar H_2O) (c), and after reduction and exposure to H_2O/H_2 = 10 (250 °C, 10 bar, 16 h, 5.5 bar H_2O) (d).
Adapted from reference [119].

metal–support compounds [175] while studies based on alumina supported catalysts followed [176,177]. A silica-supported cobalt catalyst (Co/SiO_2) was exposed to hydrothermal conditions simulating FT synthesis [175]. Steam was introduced externally for the simulation. It was found from TPR that hardly reducible species were formed upon exposure. These species were reduction resistant up to 900 °C. The authors proposed that the species were cobalt-silicates. It was also suggested that the presence of metallic cobalt is vital for the cobalt–support compound formation and that hydrogen may accelerate this formation.

Further insight into the causes of the cobalt–support compound formation came from a study of a $Co/\gamma\text{-}Al_2O_3$ catalyst [176]. The unpromoted catalyst was prepared by incipient wetness impregnation, reduced, exposed to hydrothermal conditions (mixture of helium and water vapours) at different temperatures and finally recalcined before TPR measurements. The results revealed that the presence of water vapour promotes cobalt aluminate formation. This has been explained by the possible hydration of the alumina which may stabilize the oxidic cobalt species and create strong interactions with the support and eventually induce its diffusion into subsurface regions. The authors emphasize the need for controlling the partial pressure of steam at temperatures above 150 °C, where highly dispersed Co^{2+} or metallic Co are present, in order to prevent cobalt–support compound formation. Zirconia modified alumina supported catalysts were also used in FTS. Past studies had shown that zirconia apart from good mechanical strength appears to have promotional effects on the reaction rate and the metal reducibility [177]. The examined catalysts contained 2–11 wt% ZrO_2, which was firstly impregnated on alumina, then calcined and subsequently impregnated with cobalt. FTS was carried out under differential conditions (220 °C, 1.01 bar, CO conversion <5% and H_2/CO ratio of 2) in a fixed-bed reactor. Raman spectroscopy was employed for detection of the cobalt–support mixed compounds. Reduced and passivated catalyst samples, with and without Zr modification were characterized. Steam-treated samples were characterized as well. It appears that there were no Raman bands linked to the formation of cobalt-alumina mixed compounds for the Zr-modified catalysts, even when water vapour was added during reduction. According to the authors, this suggests that zirconium enhances support stabilization by blocking defects and subsequently minimize the impact of water vapour during reduction, possibly by partially blocking cobalt-aluminate formation.

A similar effect of zirconium promotion in the cobalt–support compound formation has been reported in earlier studies [178] when zirconium oxide chloride was added to a Co/SiO_2 catalyst. TPR studies reveal that zirconium appears to lower the interaction of cobalt with the silica support. This results in a catalyst with higher reducibility, since the formed cobalt–zirconium species can be reduced at lower temperatures than cobalt silicates.

Extended model studies simulating high partial pressures of steam in FTS reactors have been performed by Holmen and co-workers. Although these studies were focusing on better understanding of the effect of water, interesting information about the strong interaction between cobalt and the alumina support were obtained [116] by using TPR, XPS and gravimetric techniques [119]. Based on the assumption of the similarity of Fischer–Tropsch reaction environment and gaseous mixtures of hydrogen and steam, model studies were carried out. Rhenium promoted and unpromoted $Co/\gamma\text{-}Al_2O_3$ reduced catalysts were exposed to H_2O/He and H_2O/H_2 mixtures and analyzed. TPR results indicated the presence of a phase which was reduced at temperatures similar to those of cobalt-aluminate compounds, i.e. 800 °C as shown in Fig. 14.

The measurements were performed after exposure of the reduced catalyst to a H_2O/He mixture at 250 °C and 10 bar. At such conditions no high temperature reduction peaks were detected for the unpromoted catalyst. After H_2O/H_2 treatment, both the Re-promoted and unpromoted catalysts showed reduction peaks at temperatures >727 °C, most likely corresponding to metal–support mixed compounds. Gravimetric measurements were used to follow the weight changes during gas mixture exposures of the catalysts. TPR results are in agreement with the reported gravimetric results in terms of oxygen uptake. Promoted catalysts appear to have a higher tendency to oxidize than their unpromoted counterparts. It was also shown that the H_2O/He treatment of the reduced catalyst led to a large increase in reduction temperatures [117]. It was sug-

gested that the cobalt oxide formed from the treatment interacts more strongly with the alumina support. This reduction difficulty is usually observed for bulk cobalt aluminate or cobalt ions having a high number of O–Al ligands (827–927 °C). In addition, in the XPS spectrum the cobalt oxide peak was dominating also after reduction, which indicates the existence of multiple cobalt compounds on the surface having widely different dispersion and reducibility.

In accordance with the previously mentioned results, investigations of noble metal-promoted Co/γ-Al_2O_3 catalysts have shown cobalt–support mixed compound formation during FTS. It was proposed that since bulk oxidation of cobalt by water is not thermodynamically permitted at typical FTS conditions, smaller clusters are interacting with the support and their behaviour deviate significantly from bulk cobalt metal. These clusters may undergo oxidation in the presence of water and subsequently lead to the diffusion of cobalt cations into the tetrahedral sites of the alumina lattice [156].

Ru-promoted and unpromoted 15 wt% Co/γ-Al_2O_3 catalysts were subjected to FTS conditions (19 bar, 220 °C, $H_2/CO = 2.0$ and SV = 5 SL/h gcat) in a CSTR for 1000 h [45]. Reduced/passivated fresh and used catalysts were characterized, with the assistance of model compounds, by means of EXAFS and XANES. From the analysis of the used samples it appeared that both pre-edge features and XANES derivative spectra resemble either Co_3O_4 or Co-aluminates mixed compounds. As already mentioned the thermodynamic behaviour of the small cobalt clusters may deviate significantly from the bulk and thus allow the re-oxidation of the small clusters and subsequently increase their interactions with the support leading to mixed metal–support compound formation. This route appears to be preferred over the complete oxidation to Co_3O_4. The contribution to the spectra from the Co_3O_4 can thus be excluded.

Platinum promoted 15 wt% Co/γ-Al_2O_3 catalyst was studied in a CSTR for behaviour in Fischer–Tropsch synthesis [142,147] (210 °C, 20 and 29.3 bar, $H_2/CO = 2$, 750 rpm and 30% Ar in the feed). In the study, various space velocities were applied together with external addition of water. The effect of the different steam concentrations was investigated. Samples were acquired before, during, and after H_2O addition and examined by XAS. The spectra were normalized and derivatives were obtained. XAS results strongly suggested that the irreversible loss in activity after the external introduction of steam at high concentrations led to the reaction of the cobalt clusters with the support, forming cobalt aluminate-like species. In particular XANES data showed a sharp peak rise ~5 eV after the edge, which closely resembled the sharp feature evident in cobalt aluminate, but absent in CoO. Moreover, the k^0-weighted spectra underwent changes in agreement with the formation of cobalt aluminate. The changes included increase in the Co–O coordination number, significant reduction of Co–Co coordination and formation of two peaks at the distance of 2.8 and 3.0 Å from the absorber, which are likely due to Co–Co coordination in the oxidized species. It was also observed that the CO_2 selectivity was low at low conversion levels and increased linearly with increasing CO conversion. This indicates increased water–gas shift activity in connection with the partial pressure of steam. It was suggested that another WGS active form of cobalt, such as cobalt oxide or cobalt-aluminate was formed. This is in line with the possibilities of re-oxidation or mixed-cobalt compound formation.

Rhenium promotion of a 15 wt% Co/γ-Al_2O_3 catalyst was also investigated [47]. The catalyst was used in a CSTR (220 °C, 20 bar, $H_2/CO = 2$, 750 rpm), withdrawn at various times on stream and characterized by XAS (XANES and EXAFS). XANES results revealed a strong contribution of the reduced cobalt metal and three small peaks which resembled the peaks of the cobalt-aluminate and Co_3O_4 model compounds. The peaks were more pronounced in the derivative spectra. This suggests that small fractions of the cobalt may have transformed into a FT inactive state. However, EXAFS data failed to verify these results. Jacobs et al. studied promoted and unpromoted catalysts with different metal loadings (15 wt% and 25 wt%) [148]. The low loaded catalysts, having cobalt particles between 5 and 6 nm, showed indications of cobalt-aluminate formation. The XANES derivatives showed a increasingly intense feature at 7717 eV for both catalysts, supporting the hypothesis of cobalt-aluminate formation. In general the catalysts with low loadings and hence small crystallite size appeared to be more sensitive to the partial pressure of water, leading to irreversible deactivation apparently caused by the metal–support mixed compounds.

Cobalt–support mixed oxide formation appears to be a surface or subsurface phenomena with no long range order, where cobalt atoms are randomly distributed in the support. However, X-ray diffraction studies of Ru-promoted Co/γ-Al_2O_3 spent catalyst revealed the existence of bulk aluminates [50]. The catalyst was used in a fixed-bed reactor at 220 °C, 20 bar and H_2/CO ratio of 2 for a period of 1000 h and subsequently characterized by several techniques. The authors suggested that external factors, like the partial pressure of steam were responsible for this deactivation. Cobalt re-oxidation and increased metal–support interactions leading to the formation of xCoO·$y$$Al_2O_3$ species was proposed as the dominating deactivation mechanism.

Chen et al. observed the formation of hydrated cobalt silicates on a Co/ZrO_2/SiO_2 catalyst tested for 500 h in a laboratory fixed-bed reactor (20 bar, 500 h^{-1}, $H_2/CO = 2$ in the temperature range from 186 to 191 °C). The employed techniques were XRD, FT-IR, TPR and TGA [179,180]. It was proposed that the hydrated cobalt silicate species were the main cause of deactivation of the FT catalyst and their formation was facilitated at high partial pressure of water.

2.6. Attrition

Attrition is defined as the unwanted breakdown of solid particles. The mechanisms of the attrition process include both abrasion/erosion (the process during which particle surface layers or corners are removed) and fracture (the fragmentation of particles) [6]. This fragmentation or abrasion of catalyst particles or pellets may result in the production of finer particles and possibly catalyst loss. The produced fines may influence the process operation by affecting the fluidization properties (e.g. foam formation inside the reactor), by plugging the solid–liquid separation devices (e.g. filters), and can emerge downstream and consequently contaminate the products (e.g. mixed with FT wax) as indicated in Fig. 15. The attrition phenomena are more intense in fluidized or slurry bed reactors [181]. However, slurry bubble column reactors have received a lot of attention in the recent years due to their excellent heat removal capabilities during FT reaction [182]. Thus, catalyst deactivation through attrition is of significant importance when the application of SBCR is considered.

Several techniques exist for measuring the attrition resistance of a catalyst. These are fluidized bed tests, collision tests, ultrasound tests and jet cup. The last appears to be most suitable and accurate for predicting attrition in a SBCR environment [182].

The mechanical strength of the support and the metal loading are critical parameters for the attrition resistance of the catalyst. Wei et al. studied the behaviour of different catalysts against attrition [183]. The study focused on the most common supports used for FT synthesis, i.e. alumina, silica and titania (rutile and anatase). Attrition resistance tests were performed both in a laboratory-scale SBCR under FT conditions for 10 days and by using an ultrasonic attrition testing procedure. The supports were calcined, sieved (grain size >38 μm) and subjected to the test. It appears that the attrition resistance has the following order: $Al_2O_3 > TiO_2$ (rutile) > SiO_2. The effect of cobalt loading was also studied and adding cobalt to alumina or silica increased the resistance towards attrition. However, titania supported catalyst did not

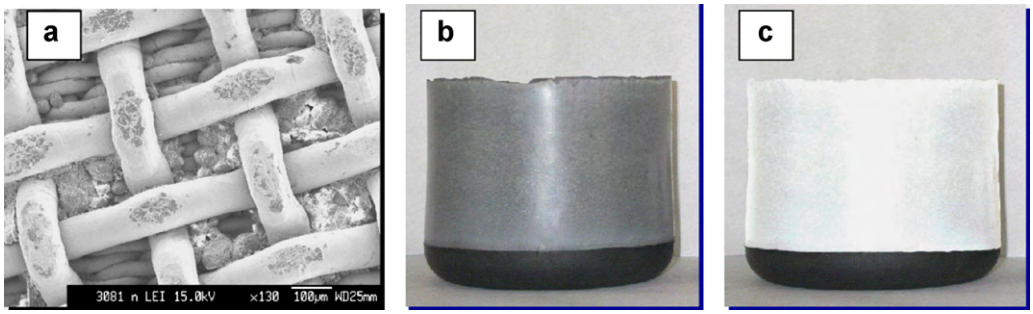

Fig. 15. Different hydrothermal behaviour of FT catalysts. (a) Settling problems and plugging of the catalyst/wax separation cartridges inside the pilot reactor, (b) after catalyst sedimentation (the black layer) the reaction product still appears gray because of the suspension of fines and (c) the reaction products for catalyst with improved hydrothermal stability.
Adapted from reference [181].

show any improvement. The catalysts had the following order of attrition resistance $Co/Al_2O_3 > Co/SiO_2 > Co/TiO_2$ (rutile) $\gg Co/TiO_2$ (anatase). Addition of metal (Ru, Cu) or oxide promoters (La, Zr, K, Cr) did not affect the attrition resistance of the catalyst significantly.

Although alumina is the most attrition resistant support, it will react with water to produce mechanically fragile hydrated forms [181] at industrial FT conditions. Suppressing attrition during Fischer–Tropsch synthesis in slurry bed reactors can be further achieved by doping of the support with various bi-valent metals (e.g. Ni) and a subsequent rise in calcination temperature of the catalyst preparation steps. In particular it appears that impregnation of alumina support with low amounts of a bi-valent metal (capable of forming a spinel compound with alumina) followed by a calcination above 550 °C and a second impregnation with the catalytically active metal increases dramatically attrition resistance of the catalyst [184].

3. Summary

A summary of the recent literature dealing with deactivation mechanisms for cobalt based Fischer–Tropsch catalysts is given below and summarized in Table 2:

(a) Poisoning is important in Fischer–Tropsch synthesis. Sulphur and possibly nitrogen contaminants are affecting catalyst performance. Purification of the feed is vital for the process and

Table 2
Proposed mechanisms of catalyst deactivation in cobalt based FTS.

Deactivation Mechanism	Short description	References
Poisoning	Sulphur in the form of H_2S, COS will poison the catalyst. Sulphur content in the feed should be kept below 0.02 mg/m^3. Feed purification is vital for the process.	[4,7,9,13–18,81]
	Nitrogen compounds appear to have a reversible poisoning effect. Other species are accused for catalyst poisoning as well.	[19–21,23,24]
Sintering	Exothermicity of the reaction dictates sintering as a possible deactivation mechanism. Coalescence seems to be the prevailing mechanism.	[26,29,38–47,49–53,55]
	Support sintering has been proposed as well.	[56]
Carbon formation and fouling	The possibility of pore plugging and catalyst fouling due to carbonaceous species formation is high, since carbon is a key element of the synthesis. The exact nature of the species is still unclear.	[4,26,59–61,80–82,84,87–98,155]
Re-oxidation	Thermodynamic calculations shown that re-oxidation is possible only for crystallites less than 5 nm in diameter. Nevertheless, several studies are proposing water-induced re-oxidation as a deactivation mechanism. In contradiction further reduction during FTS has been proposed as well.	[29,39,42,45–47,50,51,53,113–135,137–149]
	Other oxygen containing species have been investigated for their oxidizing ability.	[150–152]
Carbidization	Mainly XRD studies are reporting Co_2C formation. The formation appears to be reversible.	[46,50,55,64,75–79,153]
Metal–support solid state reactions	The formation of mixed compounds of metal and the support is thermodynamically feasible, however kinetically restricted. Water may promote this side effect.	[29,39,41,42,45,50,51,56,116,117,119,142,143,147,148,156,175–180]
Surface reconstruction	Surface reconstruction has been proposed and connected with the activation of the catalyst. Calculations have shown a link between reconstruction and deactivation, but the phenomenon is lacking experimental evidences.	[26,90,103,107–111,185]
Leaching of active phase	ICP analysis of spent catalysts used in laboratory units shows that the catalyst components are remaining in the catalyst after operation.	[5,41,42,50,51]
Attrition	Particularly valid for moving beds. Fragmentation of catalyst particles is resulting in secondary effects disturbing proper operation and assisting catalyst loss.	[181,183,184]

the levels of sulphur should be kept below 0.02 mg/m^3. Other species like alkali metals, carbon or metal carbonyls may be responsible for catalyst poisoning.

(b) Sintering is highly depended on the support. Alumina appears to stabilize cobalt crystallites and make the catalyst more resistant against sintering. However, the Hüttig temperature of Co is not far from the ordinary FT temperatures and the presence of water may accelerate sintering. In addition, crystallite transformations may increase surface mobility and enhance the possibility of agglomeration.

(c) Bulk carbidization at FT conditions, although thermodynamically not feasible, has been reported by *in situ* studies. Carbidization is reversible upon mild hydrogen treatments and this regeneration will yield *hcp* rich cobalt particles.

(d) It is expected that the formation of high molecular weight carbon species will affect the activity due to diffusion inhibition and pore plugging. It is likely that these species will accumulate and slowly undergo transformations to more stable carbon species that physically block the surface or even strongly chemisorb on the catalytically active sites. Nevertheless, this deactivation mechanism appears to be reversible with the proper treatment (i.e. solvent extraction combined with hydrogen treatment and/or calcination).

(e) It is evident that the surface of cobalt under Fischer–Tropsch conditions is dynamic and subjected to severe reconstruction. This behaviour, due to the lack of *in situ* monitoring, has rarely been taken into consideration as a cause of catalyst deactivation. However, essentially computational calculations have been performed and only recent experimental studies have evidenced surface reconstruction during FTS at low syngas partial pressures [185,109].

(f) Contradictory reports exist for the re-oxidation of cobalt FTS catalysts. Although thermodynamically not favourable, several reports are indicating surface re-oxidation. The effect is strongly linked with the presence of water. In contrast, several studies have not detected any re-oxidation. Some of them even report further reduction of the catalyst during FTS. The wide range of obtained results reveals the importance of experimental characteristics like pretreatments (i.e. calcination temperature, degree of reduction), experimental conditions (e.g. T, P, H_2/CO, GHSV, CO conversion level), catalyst micro- and macroscopic properties (crystallite size, promoter, support type and framework), instrumentation (i.e. reactors, *in situ* cells).

(g) The formation of hardly reducible cobalt–support species has been claimed by several groups. The phenomenon is highly depended on the used support and can be enhanced by the existence of surface re-oxidation. It should be noted that it cannot be the main reason of deactivation of FT catalysts since deactivation is observed also on weakly interacting supports.

(h) Attrition is an important topic for the industrial process, especially when slurry reactors are used. However, attrition is known and prevention is expected to be obtained by a balance between high calcination temperatures of doped supports with mechanical promoters and the supports surface area.

4. Concluding remarks

The present literature review of deactivation of cobalt based Fischer–Tropsch catalysts confirms the complexity of the Fischer–Tropsch reaction system. The diversity in reported opinions is evident in the majority of the proposed deactivation mechanisms. Poisoning of the catalyst and mechanical failure through attrition (mostly for slurry beds) are generally accepted. Modelling and prevention of the phenomena via catalyst design should be addressed. There is evidently a lack of information concerning the role of promoters in FTS. The nature, the state and the way noble metal promoters act under FTS conditions remains unknown and no information exist concerning their contribution to deactivation. The promoter phase transformation, segregation or alloy formation with the metal should be part of future deactivation studies. Mechanisms of deactivation that are highly dependent on the chemical environment of the reaction are still debated. Sintering, re-oxidation, cobalt–support mixed compound formation and carbon formation are the main issues. The carbon rich environment in FTS may lead to carbon species (atomic to polymeric, amorphous to crystalline) accumulating on the surface or diffusing into the bulk. Diffusion limitations may also be involved. Nevertheless, the exact nature of the carbon species and the way they act is still unclear. Although the effect of water is well documented, it is still unidentified if the effect is kinetic, diffusional or oxidative. Sintering appears to be probable under FTS conditions. Apparently, deactivation in FTS is sensitive to several parameters. By changing pretreatments, experimental conditions, catalyst micro- and macroscopic properties and instrumentation may facilitate different deactivation mechanisms. In addition, the difficulty in characterization due to the air sensitivity of metallic cobalt and the FT waxes that are covering the surface creates uncertainty in comparison of results. Thus, it is vital that well defined catalysts are studied under industrially relevant conditions with simultaneous monitoring of the involved phases. *Operando* techniques have been rapidly developed in recent years [186,187]. Application of such techniques for the Fischer–Tropsch synthesis, may facilitate the investigation of initial deactivation mechanisms by providing time resolved, accurate and quantitative information [53,55,130,188]. For long-term deactivation, extended FT runs will be beneficial and a close collaboration between industry and academia will assist towards that perspective.

Acknowledgements

This publication forms a part of the inGAP Centre of Research-based Innovation, which receives financial support from the Norwegian Research Council under contract no. 174893. The authors would like to thank the Norwegian Research Council and Statoil for financial support through the inGAP project.

References

[1] A.Y. Khodakov, W. Chu, P. Fongarland, Chem. Rev. 107 (2007) 1692–1744.
[2] E.A. Blekkan, Ø. Borg, V. Frøseth, A. Holmen, Catalysis 20 (2007) 13–32.
[3] M.E. Dry, Stud. Surf. Sci. Catal. 152 (2004) 196–257.
[4] P.J. van Berge, R.C. Everson, Stud. Surf. Sci. Catal. 107 (1997) 207–212.
[5] E. van Steen, M. Claeys, Chem. Eng. Technol. 31 (2008) 655–666.
[6] C.H. Bartholomew, Appl. Catal., A 212 (2001) 17–60.
[7] P.K. Agrawal, J.R. Katzer, W.H. Manogue, J. Catal. 69 (1981) 327–344.
[8] R.J. Farrauto, C.H. Bartholomew, Fundamentals of Industrial Catalytic Processes, 2nd edition, Wiley-Interscience, New Jersey, 2006 (Chapter 6, p. 398).
[9] R.J. Madon, H. Seaw, Catal. Rev. – Sci. Eng. 15 (1977) 69–106.
[10] M.E. Dry, Catal. Today 71 (2002) 227–241.
[11] M.E. Dry, in: J.R. Anderson, M. Boudart (Eds.), Catalysis Science and Technology, vol. 1, Springer-Verlag, New York, 1981 (Chapter 4, p. 195).
[12] M.E. Dry, Stud. Surf. Sci. Catal. 152 (2004) 533–600.
[13] C.H. Bartholomew, R.M. Bowman, Appl. Catal. 15 (1985) 59–67.
[14] A.L. Chaffee, I. Campbell, N. Valentine, Appl. Catal. 47 (1989) 253–276.
[15] V. Curtis, C.P. Nicolaides, N.J. Coville, D. Hildebrandt, D. Glasser, Catal. Today 49 (1999) 33–40.
[16] J. Li, N.J. Coville, Appl. Catal., A 208 (2001) 177–184.
[17] N.N. Madikizela-Mnqanqeni, N.J. Coville, Appl. Catal., A 340 (2008) 7–15.
[18] C.G. Visconti, L. Lietti, P. Forzatti, R. Zennaro, Appl. Catal., A 330 (2007) 49–56.
[19] S.C. LeViness, H.J. Robota, X. Zhan, J. Engman, Proc. 79th ACS Symp. Colloid and Surface Science, Potsdam, NY, 12–15 June 2005, paper 9-09.
[20] S.C. LeVinnes, C.J. Mart, W.C. Behrmann, S.J. Hsia, D.R. Neskora, WO Patent 050487 (1998) assigned to Exxon research and engineering company.
[21] S. Eri, J.G. Goodwin Jr., G. Marcelin, T. Riis, US Patent 4880763 (1989) assigned to Statoil.
[22] J. Gaube, H.F. Klein, Appl. Catal., A 350 (2008) 126–132.
[23] E. Rytter, S. Eri, WO Patent 010936 A1 (2006) assigned to Statoil ASA and Petroleum Oil & Gas Corporation of South Africa PTY.

[24] Ø. Borg, S. Eri, E.A. Blekkan, S. Storsæter, H. Wigum, E. Rytter, A. Holmen, J. Catal. 248 (2007) 89–100.
[25] M.M. Yung, W.S. Jablonski, K.A. Magrini-Bair, Energy Fuels 23 (2009) 1874–1887.
[26] A.M. Saib, D.J. Moodley, I.M. Ciobîcă, M.M. Hauman, B.H. Sigwebela, C.J. Weststrate, J.W. Niemantsverdriet, J. van de Loosdrecht, Catal. Today 154 (2010) 271–282.
[27] Y. Yin, R.M. Rioux, C.K. Erdonmez, S. Hughes, G.A. Somorjai, A.P. Alivisatos, Science 304 (2004) 711–714.
[28] P.A. Chernavskii, G.V. Pankina, V.I. Zaikovskii, N.V. Peskov, P. Afanasiev, J. Phys. Chem. C 112 (2008) 9573–9578.
[29] G. Kiss, S. Soled, C. Kliewer, Proc. 11th Int. Symp. Catalyst Deactivation, Delft, The Netherlands, 25–28 October 2009, paper O15.
[30] J.J.C. Geerlings, J.H. Wilson, G.J. Kramer, H.P.C.E. Kuipers, A. Hoek, H.M. Huisman, Appl. Catal., A 186 (1999) 27–40.
[31] C. Maretto, R. Krishna, Catal. Today 52 (1999) 279–289.
[32] Ø. Borg, P.D.C. Dietzel, A.I. Spjelkavik, E.Z. Tveten, J.C. Walmsley, S. Diplas, S. Eri, A. Holmen, E. Rytter, J. Catal. 259 (2008) 161–164.
[33] J.A. Moulijn, A.E. van Diepen, F. Kapteijn, Appl. Catal., A 212 (2001) 3–16.
[34] G. Palasantzas, T. Vystavel, S.A. Koch, J.Th.M. De Hosson, J. Appl. Phys. 99 (2006), 024307-1-5.
[35] M. Mirjalili, J. Vahdati-Khaki, J. Phys. Chem. Solids 69 (2008) 2116–2123.
[36] B. Jager, R. Espinoza, Catal. Today 23 (1995) 17–28.
[37] J.L. Casci, C.M. Lok, M.D. Shannon, Catal. Today 145 (2009) 38–44.
[38] C.J. Bertole, C.A. Mims, G. Kiss, J. Catal. 210 (2002) 84–96.
[39] G. Kiss, C.E. Kliewer, G.J. DeMartin, C.C. Culross, J.E. Baumgartner, J. Catal. 217 (2003) 127–140.
[40] S. Soled, C. Kliewer, G. Kiss, J. Baumgartner, Proc. 11th Int. Symp. 21st North American Meeting, North American Catalysis Society (NAM-NACS), San Francisco, USA, 7–11 June 2009, paper 1062.
[41] W. Zhou, J. Chen, K. Fang, Y. Sun, Fuel Process. Technol. 87 (2006) 609–616.
[42] L. Shi, J. Chen, K. Fang, Y. Sun, Stud. Surf. Sci. Catal. 167 (2007) 97–102.
[43] S. Bessell, Stud. Surf. Sci. Catal. 81 (1994) 483–486.
[44] G.-Z. Bian, N. Fujishita, T. Mochizuki, W.-S. Ning, M. Yamada, Appl. Catal., A 252 (2003) 251–260.
[45] G. Jacobs, Y. Zhang, T.K. Das, J. Li, P.M. Patterson, B.H. Davis, Stud. Surf. Sci. Catal. 139 (2001) 415–422.
[46] G. Jacobs, P.M. Patterson, Y. Zhang, T. Das, J. Li, B.H. Davis, Appl. Catal., A 233 (2002) 215–226.
[47] T.K. Das, G. Jacobs, P.M. Patterson, W.A. Conner, J. Li, B.H. Davis, Fuel 82 (2003) 805–815.
[48] A. Jentys, Phys. Chem. Chem. Phys. 1 (1999) 4059–4063.
[49] G. Jacobs, A. Sarkar, Y. Ji, M. Luo, A. Dozier, B.H. Davis, Ind. Eng. Chem. Res. 47 (2008) 672–680.
[50] A. Tavasoli, R.M. Malek Abbaslou, A.K. Dalai, Appl. Catal., A 346 (2008) 58–64.
[51] A. Tavasoli, M. Irani, R.M. Malek Abbaslou, M. Trepanier, A.K. Dalai, Can. J. Chem. Eng. 86 (2008) 1070–1080.
[52] M.J. Overett, B. Breedt, E. du Plessis, W. Erasmus, J. van de Loosdrecht, Prepr. Pap.-Am. Chem. Soc., Div. Petr. Chem. 53 (2008) 126–128.
[53] M. Rønning, N.E. Tsakoumis, A. Voronov, R.E. Johnsen, P. Norby, W. van Beek, Ø. Borg, E. Rytter, A. Holmen, Catal. Today, doi:10.1016/j.cattod.2009.10.010.
[54] J.-D. Grunwaldt, B.S. Clausen, Top. Catal. 18 (2002) 37–43.
[55] H. Karaca, J. Hong, P. Fongarland, P. Roussel, A. Griboval-Constant, M. Lacroix, K. Hortmann, O. Safonova, A.Y. Khodakov, Proc. EUROPACAT IX Congress, Salamanca, Spain, 30/08 to 04/09 2009, paper O11-6.
[56] G.W. Huber, C.G. Guymon, T.L. Conrad, B.C. Stephenson, C.H. Bartholomew, Stud. Surf. Sci. Catal. 139 (2001) 423–430.
[57] P.G. Menon, J. Mol. Catal. 59 (1990) 207–220.
[58] C.H. Bartholomew, Catal. Rev. – Sci. Eng. 24 (1982) 67–112.
[59] D.J. Moodley, J. van de Loosdrecht, A.M. Saib, J.W. Niemantsverdriet, Prepr. Pap.-Am. Chem. Soc., Div. Petr. Chem. 53 (2008) 122–125.
[60] D.-K. Lee, J.-H. Lee, S.-K. Ihm, Appl. Catal. 36 (1988) 199–207.
[61] D.J. Moodley, J. van de Loosdrecht, A.M. Saib, M.J. Overett, A.K. Datye, J.W. Niemantsverdriet, Appl. Catal., A 354 (2009) 102–110.
[62] A. Barbier, A. Tuel, I. Arcon, A. Kodre, G.A. Martin, J. Catal. 200 (2001) 106–116.
[63] L.J.E. Hofer, W.C. Peebles, J. Am. Chem. Soc. 69 (1947) 893–899.
[64] O. Ducreux, J. Lynch, B. Rebours, M. Roy, P. Chaumette, Stud. Surf. Sci. Catal. 119 (1998) 125–130.
[65] S. Nagakura, J. Phys. Soc. Jpn. 16 (1961) 1213–1219.
[66] F. Tihay, G. Pourroy, M. Richard-Plouet, A.C. Roger, A. Kiennemann, Appl. Catal., A 206 (2001) 29–42.
[67] E. de Smit, B.M. Weckhuysen, Chem. Soc. Rev. 37 (2008) 2758–2781.
[68] S. Storsæter, D. Chen, A. Holmen, Surf. Sci. 600 (2006) 2051–2063.
[69] E. Shustorovich, A.T. Bell, Surf. Sci. 248 (1991) 359–368.
[70] B.H. Davis, Fuel Process. Technol. 71 (2001) 157–166.
[71] S. Weller, L.J.E. Hofer, R.B. Anderson, J. Am. Chem. Soc. 70 (1948) 799–801.
[72] L.C. Browning, P.H. Emmett, J. Am. Chem. Soc. 74 (1952) 1680–1682.
[73] O. Ducreux, B. Rebours, J. Lynch, M. Roy-Auberger, D. Bazin, Oil Gas Sci. Technol. 64 (2009) 49–62.
[74] D.I. Enache, B. Rebours, M. Roy-Auberger, R. Revel, J. Catal. 205 (2002) 346–353.
[75] P.K. Agrawal, J.R. Katzer, W.H. Manogue, J. Catal. 69 (1981) 312–326.
[76] V. Gruver, X. Zhan, J. Engman, H.J. Robota, S.L. Suib, M. Polverejan, Prepr. Pap.-Am. Chem. Soc., Div. Petr. Chem. 49 (2004) 192–194.
[77] J. Xiong, Y. Ding, T. Wang, L. Yan, W. Chen, H. Zhu, Y. Lu, Catal. Lett. 102 (2005) 265–269.
[78] H.W. Pennline, S.S. Pollack, Ind. Eng. Chem. Prod. Res. Dev. 25 (1980) 11–14.
[79] H.W. Pennline, R.J. Gormley, R.R. Schehl, Ind. Eng. Chem. Prod. Res. Dev. 23 (1984) 393–404.
[80] M.K. Niemelä, A.O.I. Krause, Catal. Lett. 42 (1996) 161–166.
[81] M.S. Kim, N.M. Rodriguez, R.T.K. Baker, J. Catal. 143 (1993) 449–463.
[82] J.J.H.M. Font Freide, T.D. Gamlin, J.R. Hensman, B. Nay, C. Sharp, J. Nat. Gas Chem. 13 (2004) 1–9.
[83] R.M. Bowman, C.H. Bartholomew, Appl. Catal. 7 (1983) 179–187.
[84] E. Iglesia, S.L. Soled, R.A. Fiato, G.H. Via, Stud. Surf. Sci. Catal. 81 (1994) 433–442.
[85] A. Oberlin, M. Endo, T. Koyama, J. Cryst. Growth 32 (1976) 335–349.
[86] R.T.K. Baker, Carbon 27 (1989) 315–323.
[87] L. Borkó, Z.E. Horváth, Z. Schay, L. Guczi, Stud. Surf. Sci. Catal. 167 (2007) 231–236.
[88] J.W. Bae, S.-M. Kim, S.-J. Park, P.S.S. Prasad, Y.-J. Lee, K.-W. Jun, Ind. Eng. Chem. Res. 48 (2009) 3228–3233.
[89] J. Lahtinen, G.A. Somorjai, J. Mol. Catal. A: Chem. 130 (1998) 255–260.
[90] K.F. Tan, J. Xu, J. Chang, A. Borgna, M. Saeys, Deactivation and Promotion of Co Catalysts During Fischer-Tropsch Synthesis: a Computational and Experimental Study, *AIChE Annual Meeting* Nashville, 10 November (2009) http://aiche.confex.com/aiche/2009/webprogram/Paper161194.html.
[91] R.M.M. Abbaslou, J.S.S. Mohammadzadeh, A.K. Dalai, Fuel Process. Technol. 90 (2009) 849–856.
[92] J. He, Z. Liu, Y. Yoneyama, N. Nishiyama, N. Tsubaki, Chem. Eur. J. 12 (2006) 8296–8304.
[93] X. Li, J. He, M. Meng, Y. Yoneyama, N. Tsubaki, J. Catal. 265 (2009) 26–34.
[94] J.J.C. Geerlings, M.C. Zonnevylle, C.P.M. de Groot, Surf. Sci. 241 (1991) 315–324.
[95] J.J.C. Geerlings, M.C. Zonnevylle, C.P.M. de Groot, Surf. Sci. 241 (1991) 302–314.
[96] M.C. Zonnevylle, J.J.C. Geerlings, R.A. van Santen, Surf. Sci. 240 (1990) 253–262.
[97] J.C.W. Swart, I.M. Ciobîcă, R.A. van Santen, E. van Steen, J. Phys. Chem. C 112 (2008) 12899–12904.
[98] J.C.W. Swart, E. van Steen, I.M. Ciobîcă, R.A. van Santen, Phys. Chem. Chem. Phys. 11 (2009) 803–807.
[99] G.A. Somorjai, M.A. van Hove, Prog. Surf. Sci. 30 (1989) 201–231.
[100] H.P. Bonzel, H.J. Krebs, Surf. Sci. 117 (1982) 639–658.
[101] J. Wilson, C. de Groot, J. Phys. Chem. 99 (1995) 7860–7866.
[102] G.A. Beitel, A. Laskov, H. Oosterbeek, E.W. Kuipers, J. Phys. Chem. 100 (1996) 12494–12502.
[103] G.A. Beitel, C.P.M. de Groot, H. Oosterbeek, J.H. Wilson, J. Phys. Chem. B 101 (1997) 4035–4043.
[104] H.J. Venvik, A. Borg, C. Berg, Surf. Sci. 397 (1998) 322–332.
[105] H.J. Venvik, C. Berg, A. Borg, Surf. Sci. 402–404 (1998) 57–61.
[106] G. Rupprechter, C. Weilach, J. Phys.: Condens. Matter 20 (2008) 184019.
[107] H. Schulz, Z. Nie, F. Ousmanov, Catal. Today 71 (2002) 351–360.
[108] H. Schulz, Top. Catal. 26 (2003) 73–85.
[109] G.L. Bezemer, J.H. Bitter, H.P.C.E. Kuipers, H. Oosterbeek, J.E. Holewijn, X. Xu, F. Kapteijn, A.J. van Dillen, K.P. de Jong, J. Am. Chem. Soc. 128 (2006) 3956–3964.
[110] Q. Ge, M. Neurock, J. Phys. Chem. B 110 (2006) 15368–15380.
[111] I.M. Ciobîcă, R.A. van Santen, P.J. van Berge, J. van de Loosdrecht, Surf. Sci. 602 (2008) 17–27.
[112] E. Iglesia, Appl. Catal., A 161 (1997) 59–78.
[113] J. van de Loosdrecht, B. Balzhinimaev, J.-A. Dalmon, J.W. Niemantsverdriet, S.V. Tsybulya, A.M. Saib, P.J. van Berge, J.L. Visagie, Catal. Today 123 (2007) 293–302.
[114] A.K. Dalai, B.H. Davis, Appl. Catal., A 348 (2008) 1–15.
[115] E. van Steen, M. Claeys, M.E. Dry, J. van de Loosdrecht, E.L. Viljoen, J.L. Visagie, J. Phys. Chem. B 109 (2005) 3575–3577.
[116] D. Schanke, A.M. Hilmen, E. Bergene, K. Kinnari, E. Rytter, E. Ådnanes, A. Holmen, Catal. Lett. 34 (1995) 269–284.
[117] D. Schanke, A.M. Hilmen, E. Bergene, K. Kinnari, E. Rytter, E. Ådnanes, A. Holmen, Energy Fuels 10 (1996) 867–872.
[118] M. Rothaemel, K.F. Hanssen, E.A. Blekkan, D. Schanke, A. Holmen, Catal. Today 38 (1997) 79–84.
[119] A.M. Hilmen, D. Schanke, K.F. Hanssen, A. Holmen, Appl. Catal., A 186 (1999) 169–188.
[120] A.M. Hilmen, D. Schanke, A. Holmen, Stud. Surf. Sci. Catal. 107 (1997) 237–242.
[121] A.M. Hilmen, O.A. Lindvåg, E. Bergene, D. Schanke, S. Eri, A. Holmen, Stud. Surf. Sci. Catal. 136 (2001) 295–300.
[122] S. Storsæter, B. Tøtdal, J.C. Walmsley, B.S. Tanem, A. Holmen, J. Catal. 236 (2005) 139–152.
[123] S. Storsæter, Ø. Borg, E.A. Blekkan, B. Tøtdal, A. Holmen, Catal. Today 100 (2005) 343–347.
[124] S. Storsæter, Ø. Borg, E.A. Blekkan, A. Holmen, J. Catal. 231 (2005) 405–419.
[125] Ø. Borg, S. Storsæter, S. Eri, H. Wigum, E. Rytter, A. Holmen, Catal. Lett. 107 (2006) 95–102.
[126] G.P. Huffman, N. Shah, J.M. Zhao, F.E. Huggins, T.E. Hoost, S. Halvorsen, J.G. Goodwin, J. Catal. 151 (1995) 17–25.
[127] F.W. Lytle, P.S.P. Wei, R.B. Greegor, G.H. Via, J.H. Sinfelt, J. Chem. Phys. 70 (1979) 4849–4855.
[128] P.J. van Berge, J. van de Loosdrecht, S. Barradas, A.M. van der Kraan, Catal. Today 58 (2000) 321–334.
[129] J. van de Loosdrecht, P.J. van Berge, M.W.J. Crajé, A.M. van der Kraan, Hyperfine Interact. 139–140 (2002) 3–18.
[130] M.W.J. Crajé, A.M. van der Kraan, J. van de Loosdrecht, P.J. van Berge, Catal. Today 71 (2002) 369–379.

[131] A.M. Saib, A. Borgna, J. van de Loosdrecht, P.J. van Berge, J.W. Niemantsverdriet, J. Phys. Chem. B 110 (2006) 8657–8664.
[132] A.M. Saib, A. Borgna, J. van de Loosdrecht, P.J. van Berge, J.W. Geus, J.W. Niemantsverdriet, J. Catal. 239 (2006) 326–339.
[133] A.M. Saib, A. Borgna, J. van de Loosdrecht, P.J. van Berge, J.W. Niemantsverdriet, Appl. Catal., A 312 (2006) 12–19.
[134] F.G. Botes, Ind. Eng. Chem. Res. 48 (2009) 1859–1865.
[135] S. Krishnamoorthy, M. Tu, M.P. Ojeda, D. Pinna, E. Iglesia, J. Catal. 211 (2002) 422–433.
[136] C.K. Kliewer, G. Kiss, G.J. DeMartin, Microsc. Microanal. 12 (2006) 135–144.
[137] A.K. Dalai, T.K. Das, K.V. Chaudhari, G. Jacobs, B.H. Davis, Appl. Catal., A 289 (2005) 135–142.
[138] T.K. Das, X. Zhan, J. Li, G. Jacobs, M.E. Dry, B.H. Davis, Stud. Surf. Sci. Catal. 163 (2007) 289–312.
[139] T.K. Das, W. Conner, G. Jacobs, J. Li, K. Chaudhari, Burtron H. Davis, Stud. Surf. Sci. Catal. 147 (2004) 331–336.
[140] T.K. Das, W.A. Conner, J. Li, G. Jacobs, M.E. Dry, B.H. Davis, Energy Fuels 19 (2005) 1430–1439.
[141] G. Jacobs, T.K. Das, J. Li, M. Luo, P.M. Patterson, B.H. Davis, Stud. Surf. Sci. Catal. 163 (2007) 217–253.
[142] J. Li, X. Zhan, Y. Zhang, G. Jacobs, T. Das, B.H. Davis, Appl. Catal., A 228 (2002) 203–212.
[143] J. Li, G. Jacobs, T. Das, B.H. Davis, Appl. Catal., A 233 (2002) 255–262.
[144] J. Li, G. Jacobs, T. Das, Y. Zhang, B.H. Davis, Appl. Catal., A 236 (2002) 67–76.
[145] J. Li, B.H. Davis, Stud. Surf. Sci. Catal. 147 (2004) 307–312.
[146] Y. Zhang, G. Jacobs, D.E. Sparks, M.E. Dry, B.H. Davis, Catal. Today 71 (2002) 411–418.
[147] G. Jacobs, T.K. Das, P.M. Patterson, J. Li, L. Sanchez, B.H. Davis, Appl. Catal., A 247 (2003) 335–343.
[148] G. Jacobs, P.M. Patterson, T.K. Das, M. Luo, B.H. Davis, Appl. Catal., A 270 (2004) 65–76.
[149] A.Y. Khodakov, Catal. Today 144 (2009) 251–257.
[150] S.-M. Kim, J.W. Bae, Y.-J. Lee, K.-W. Jun, Catal. Commun. 9 (2008) 2269–2273.
[151] W. Zhou, Z. Ma, K. Fang, J. Chen, Y. Sun, Fuel Process. Technol. 89 (2008) 1113–1120.
[152] K. Jalama, N.J. Coville, D. Hildebrandt, D. Glasser, L.L. Jewell, Fuel 86 (2007) 73–80.
[153] B. Ernst, A. Bensaddik, L. Hilaire, P. Chaumette, A. Kiennemann, Catal. Today 39 (1998) 329–341.
[154] T. Herranz, X. Deng, A. Cabot, J. Guo, M. Salmeron, J. Phys. Chem. B 113 (2009) 10721–10727.
[155] Z. Yan, Z. Wang, D.B. Bukur, D.W. Goodman, J. Catal. 268 (2009) 196–200.
[156] G. Jacobs, T.K. Das, Y. Zhang, J. Li, G. Racoillet, B.H. Davis, Appl. Catal., A 233 (2002) 263–281.
[157] L.B. Backman, A. Rautiainen, A.O.I. Krause, M. Lindblad, Catal. Today 43 (1998) 11–19.
[158] J.T. Richardson, L.W. Vernon, J. Phys. Chem. 62 (1958) 1153–1157.
[159] R.L. Chin, D.M. Hercules, J. Phys. Chem. 86 (1982) 360–367.
[160] R.B. Greegor, F.W. Lytle, R.L. Chin, D.M. Hercules, J. Phys. Chem. 85 (1981) 1232–1235.
[161] J.M. Jabłoński, M. Wołcyrz, L. Krajczyk, J. Catal. 173 (1998) 530–534.
[162] B. Ernst, S. Libs, P. Chaumette, A. Kiennemann, Appl. Catal., A 186 (1999) 145–168.
[163] P. Arnoldy, J.A. Moulijn, J. Catal. 93 (1985) 38–54.
[164] W.-J. Wang, Y.-W. Chen, Appl. Catal. 77 (1991) 223–233.
[165] H. Ming, B.G. Baker, Appl. Catal., A 123 (1995) 23–36.
[166] M. Rønning, D.G. Nicholson, A. Holmen, Catal. Lett. 72 (2001) 141–146.
[167] K.E. Coulter, A.G. Sault, J. Catal. 154 (1995) 56–64.
[168] P.H. Bolt, F.H.P.M. Habraken, J.W. Geus, J. Solid State Chem. 135 (1998) 59–69.
[169] W. Chu, P.A. Chernavskii, L. Gengembre, G.A. Pankina, P. Fongarland, A.Y. Khodakov, J. Catal. 252 (2007) 215–230.
[170] B. Jongsomjit, J. Panpranot, J.G. Goodwin Jr., J. Catal. 204 (2001) 98–109.
[171] A. Moen, D.G. Nicholson, M. Rønning, H. Emerich, J. Mater. Chem. 8 (1998) 2533–2539.
[172] A. Moen, D.G. Nicholson, B.S. Clausen, P.L. Hansen, A. Molenbroek, G. Steffensen, Chem. Mater. 9 (1997) 1241–1247.
[173] X.X. Gao, C.J. Huang, N.W. Zhang, J.H. Li, W.Z. Weng, H.L. Wan, Catal. Today 131 (2008) 211–218.
[174] A. Moen, D.G. Nicholson, M. Rønning, G.M. Lamble, J.-F. Lee, H. Emerich, J. Chem. Soc., Faraday Trans. 93 (1997) 4071–4077.
[175] A. Kogelbauer, J.C. Weber, J.G. Goodwin Jr., Catal. Lett. 34 (1995) 259–267.
[176] A. Sirijaruphan, A. Horvath, J.G. Goodwin Jr., R. Oukaci, Catal. Lett. 91 (2003) 89–94.
[177] B. Jongsomjit, J. Panpranot, J.G. Goodwin Jr., J. Catal. 215 (2003) 66–77.
[178] A. Feller, M. Claeys, E. van Steen, J. Catal. 185 (1999) 120–130.
[179] J.-G. Chen, X.-Z. Wang, H.-W. Xiang, Y.-H. Sun, Stud. Surf. Sci. Catal. 136 (2001) 525–529.
[180] J.-G. Chen, H.-W. Xiang, H.-Y. Gao, Y.-H. Sun, React. Kinet. Catal. Lett. 73 (2001) 169–177.
[181] C. Perego, R. Bortolo, R. Zennaro, Catal. Today 142 (2009) 9–16.
[182] R. Zhao, J.G. Goodwin Jr., R. Oukaci, Appl. Catal., A 189 (1999) 99–116.
[183] D. Wei, J.G. Goodwin Jr., R. Oukaci, A.H. Singleton, Appl. Catal., A 210 (2001) 137–150.
[184] E. Rytter, T.H. Skagseth, H. Wigum, WO Patent 072866 A1 (2005) assigned to Statoil ASA and PetroSA.
[185] G. Prieto, A. Martínez, P. Concepción, R. Moreno-Tost, J. Catal. 266 (2009) 129–144.
[186] B.M. Weckhuysen, Phys. Chem. Chem. Phys. 5 (2003) 4351–4360.
[187] H. Topsøe, J. Catal. 216 (2003) 155–164.
[188] M. Claeys, S. Kelly, E. van Steen, J. Visagie, J. van de Loosdrecht, I. Krylov, Proc. 3rd Int. Congress on Operando Spectroscopy, Rostock-Warnemünde, Germany, 19–23 April 2009, paper P4-08.